



Histological study on side effects and tumor targeting of a block copolymer micelle on rats

Takanori Kawaguchi^{a,b}, Takashi Honda^b, Masamichi Nishihara^c,
Tatsuhiko Yamamoto^c, Masayuki Yokoyama^{c,*}

^a Department of Pathology, Aizu Central Hospital, Aizu Wakamatsu 965-8611, Japan

^b Division of Human Life Sciences, Fukushima Medical University School of Nursing, Hilariga-oka 1, Fukushima, Fukushima 960-1295, Japan

^c Yokoyama Project, Kanagawa Academy of Science and Technology, KSP East 404, Sakado 3-2-1, Takatsu-ku, Kawasaki, Kanagawa 213-0012, Japan

ARTICLE INFO

Article history:

Received 11 September 2008

Accepted 12 February 2009

Available online xxx

Keywords:

Polymeric micelle

Pathology

Side effects

Block copolymer

Targeting

ABSTRACT

Histological examinations were performed with polymeric micelle-injected rats for evaluations of possible toxicities of polymeric micelle carriers. Weight of major organs as well as body weight of rats was measured after multiple intravenous injections of polymeric micelles forming from poly(ethylene glycol)-*b*-poly(aspartate) block copolymer. No pathological toxic side effects were observed at two different doses, followed only by activation of the mononuclear phagocyte system (MPS) in the spleen, liver, lung, bone marrow, and lymph node. This finding confirms the absence of - or the very low level of - *in vivo* toxicity of the polymeric micelle carriers that were reported in previous animal experiments and clinical results. Then, immunohistochemical analyses with a biotinylated polymeric micelle confirmed specific accumulation of the micelle in the MPS. The immunohistochemical analyses also revealed, first, very rapid and specific accumulation of the micelle in the vasculatures of tumor capsule of rat ascites hepatoma AH109A, and second, the micelle's scanty infiltration into tumor parenchyma. This finding suggests a unique tumor-accumulation mechanism that is very different from simple EPR effect-based tumor targeting.

© 2009 Published by Elsevier B.V.

1. Introduction

Recently, block copolymer micelles have gained considerable attentions as an efficacious carrier system of anti-cancer drugs [1-4]. Two objectives have been pursued with the polymeric micelle carriers; solubilization of water-insoluble drugs and targeting to solid tumors. Owing to a large loading capacity of the polymeric micelles, inner core for hydrophobic drugs, the polymeric micelles facilitate easy and safe intravenous injections of water-insoluble drugs such as paclitaxel [5,6]. The second objective, the targeting of the polymeric micelle carrier systems to solid tumors, is achieved by the targeting through the EPR (enhanced permeability and retention) effect [7,8]. For effective utilization of the EPR effect, poly(ethylene glycol) (PEG) has been used as an outer-shell-forming polymer block owing to its inert characteristics in interactions and uptake with or by bio-components such as proteins and cells. In particular, the PEG outer shell of the micelle is considered a critical factor in the reduction of micelle uptake by the mononuclear phagocyte system (MPS). For several anti-cancer drugs such as doxorubicin [2], cisplatin [9], and paclitaxel [10], the tumor targeting was successfully achieved in solid-tumor models in

mouse. Research reported that, accompanying this targeting effect were diminished toxic side effects of the incorporated anti-cancer drugs; specifically, a reduction of nephrotoxicity [11] and pulmonary toxicity [12]. Furthermore, a paclitaxel-incorporating polymeric micelle enhanced the radiosensitizing activity of the drug [13]. Following these good results in animal evaluations, four clinical trials of polymeric micelle targeting are underway in 2008 for doxorubicin [14] paclitaxel [15], cisplatin [9], and SN-38 [16,17], the last of which is an active species of CPT-11.

The targeting efficiency and the toxic side effects of a given carrier are two important issues for drug targeting. In the "animal-tumor model" studies and the clinical-trial results mentioned above, carrier-based toxicities were not observed. In other words, the conclusion was that all the observed toxic side effects in animals and humans had resulted from either the anti-cancer drug delivered to normal organs and tissues or the drug released from the polymeric micelle carrier during its circulation in the bloodstream. Research has frequently noted the presence of carrier-based toxic side effects in drug targeting systems, and these side effects have included the hand-foot syndrome for a doxorubicin-incorporating liposome [18] and the infusion-related reactions for an antibody-anti-cancer drug conjugate [19]. These adverse effects can be a major concern in their clinical uses. Therefore, no or low toxicity in the polymeric micelle carriers seems a great advantage. Although the polymeric micelle systems are considered

* Corresponding author. Tel.: +81 44 819 2093; fax: +81 44 819 2095.
E-mail address: yp.yokoyama2093ryo@newcast.or.jp (M. Yokoyama).

very safe carriers at least for anti-cancer drugs, it is worth while to conduct detailed histological and immunohistological examinations to identify the exact profiles and the exact mechanisms of the polymeric micelle carriers' possible toxic side effects. It is believed that these examinations can contribute not only to increasingly refined polymeric micelle designs for anti-cancer drug targeting, but also to polymeric micelles' applications to drugs other than anti-cancer drugs. In general, non-anti-cancer drugs exhibit milder toxic side effects than anti-cancer drugs. Even if carriers possess a low level of toxic side effects, these side effects may not be detected in the presence of strong toxic side effects of anti-cancer drugs. In such circumstance, it is not so important to examine the carriers' toxic effects in detail. In contrast, the carriers' toxic effects may be easily detected and be a problem in carriers' applications to non-anti-cancer-drugs that exhibit much milder side effects than anti-cancer drugs. Therefore, greater details in carriers' toxicity observation may be required for drug carriers' application to the non-anti-cancer drugs.

Concerning *in vivo* activities of polymeric micelles or of micelle-forming block copolymers, two interesting phenomena were reported: the depletion-of-ATP phenomenon and ABC (accelerated blood clearance) phenomenon. Kabanov et al. reported that Pluronic block polymers (poly(ethylene oxide)-*b*-poly(propylene oxide)-*b*-poly(ethylene oxide) block copolymers) could inhibit the activity of the protein playing a major role in multi-drug resistance through an ATP depletion mechanism [20,21]. The second ABC phenomenon is that clearance of long-circulating drug carriers is enhanced at the second dose through an immunological action. This phenomenon was reported by Dams et al. [22] and by Ishida et al. [23,24] for PEG-coated liposomes. Recently, this ABC phenomenon was also observed for a polymeric micelle carrier [25]. Therefore, it is challenging and interesting to examine detailed biological activities of PEG-based polymeric micelles whose distinctive activities or toxicities cannot be found in simple *in vivo* tests. No histological examinations, however, have been conducted for the polymeric micelle carriers that do not load any drug.

The current study analyzes acute biological activities of polymeric micelles forming from poly(ethylene glycol)-*b*-poly(aspartate) block copolymers that achieved successful tumor targeting of an anti-cancer agent camptothecin [26,27] and targeting of all-trans retinoic acid [28] by incorporation of these agents into the micelle. In this study, a term 'acute' is used to indicate a term of several weeks after the micelle injection. Therefore, the biological analysis is carried out for 30 days in the longest case. This study measured weight change of the whole body and major organs, and preformed histopathological observations with rats. Furthermore, a biotinylated polymeric micelle was prepared, and its

Table 1

Weights of major organs after polymeric micelle injections

Dose	20 mg/kg × 5 ^{a)}			200 mg/kg × 5 ^{b)}		
	Polymeric micelle	Control ^{c)}	Statistical significance ^{d)}	Polymeric micelle	Control ^{c)}	Statistical significance ^{d)}
Brain	1.36 ± 0.06	1.35 ± 0.09	n.s. ^{e)}	1.65 ± 0.10	1.57 ± 0.10	n.s. ^{e)}
Heart	0.95 ± 0.09	0.89 ± 0.09	n.s.	0.58 ± 0.06	0.67 ± 0.07	n.s.
Lung	1.33 ± 0.11	1.27 ± 0.19	n.s.	1.21 ± 0.08	1.44 ± 0.12	n.s.
Liver	18.18 ± 1.47	16.80 ± 2.09	n.s.	10.60 ± 1.08	10.55 ± 0.67	n.s.
Spleen	0.70 ± 0.09	0.64 ± 0.10	n.s.	0.37 ± 0.06	0.46 ± 0.07	n.s.
Kidney	2.47 ± 0.20	2.39 ± 0.16	n.s.	1.61 ± 0.16	1.73 ± 0.16	n.s.

^{a)} Injections on days 0,1,3,5, and 7. Weights of organs were measured on day 30.

^{b)} Injections on days 0,1,2,3, and 4. Weights of organs were measured on day 7.

^{c)} Injections of physiological saline.

^{d)} By Student's *t*-test. Difference is considered significant when *p* < 0.05.

^{e)} n.s.: not significant.

tissue/cell distribution was analyzed with tumor-bearing rats. These evaluations and analyses provide valuable information on toxicity profiling of the polymeric micelle carriers, and may yield deep insight into polymeric micelles' targeting mechanism at solid-tumor sites.

2. Materials and methods

2.1. Preparation of block copolymer micelle

Two block copolymers were synthesized. Their chemical structures are shown in Fig. 1. One block copolymer is poly(ethylene glycol)-*b*-poly(aspartate) (PEG-*P*(Asp(Bzl))), which possesses both a hydrophilic aspartic acid residue and a hydrophobic benzyl aspartate residue in one polymer block. This block copolymer was synthesized according to a previously reported method [29]. As summarized in Table 1, the PEG chain's average molecular weight of this block copolymer was 5200, and the average number of the Asp units was 24. The benzyl ester content was 89% with respect to the Asp unit. The other block copolymer is biotinyl-poly(ethylene glycol)-*b*-poly(benzyl aspartate) (biotin-PEG-*P*(Asp(Bzl))), which possesses almost the same composition as that of PEG-*P*(Asp(Bzl)) except that the former features the terminal biotin moiety. In the current study, this biotinylated polymer was prepared according to the same method [29] with some modifications in the biotinylation at a polymer terminal. The starting material for this synthesis was α -amino propyl- ω -3,3'-diethoxypropyloxy poly(ethylene glycol) (acetal-PEG-NH₂). The average molecular weight of this PEG block was 4900. Detailed synthetic procedures will be published elsewhere. In brief, the biotinylation was conducted according to a Schiff-base formation between the terminal aldehyde group and a biotinylation reagent, 5-(biotinamido)pentylamine (Pierce Biotechnology, Inc., Rockford, IL). The formed Schiff-base was reduced with sodium cyanoborohydride to obtain a stable secondary amine group as shown in Fig. 1. The obtained biotin-PEG-*P*(Asp(Bzl)) was characterized by means of ¹H NMR spectroscopy. From a ¹H NMR spectrum, conjugation of the biotin residue at the polymer terminal was found quantitatively (104%), and the benzyl ester content at the aspartic acid residue was determined to be 82%. The number of the aspartic acid residue was 25, and the molecular weight of this biotin-PEG-*P*(Asp(Bzl)) was 9700, as summarized in Fig. 1.

A polymeric micelle solution was prepared by means of a solvent- evaporation method as described previously [17]. The block copolymer was dissolved in chloroform. The solution was stirred in a glass bottle under a dry N₂ flow, allowing for evaporation of chloroform. Then, water was added to the dried residue, and sonication was applied so that a dispersed micelle solution would result. "Block copolymer micelle" solutions were stored at -30 °C until use. In non-biotinylated polymeric micelle preparations for toxicity evaluations, PEG-*P*(Asp(Bzl)) was used. In biotinylated micelle preparations, 10 mol% of biotin-PEG-*P*(Asp(Bzl)) and 90 mol% of (non-biotinylated) 160

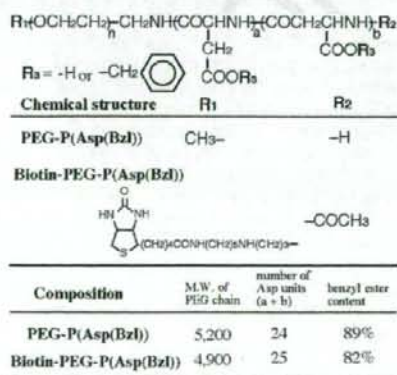


Fig. 1. Chemical structures and compositions of PEG-*P*(Asp(Bzl)) and biotin-PEG-*P*(Asp(Bzl)) block copolymers.

161 PEG-P(Asp(Bzl)) (molecular weight of the PEG chain: 5200, number of
162 Asp units: 24, benzyl ester content: 89%, and total molecular weight:
163 9800) were mixed and applied to the evaporation method.

164 2.2. Animal tests

165 2.2.1. Animals

166 Four-week-old to six-week-old female Donryu strain rats (60–80 g)
167 were purchased from Chares River (Tokyo, Japan). The rats were
168 maintained under water ad libitum and were used for experiments
169 when they grew to 120–160 g. All animal experiments were carried out
170 under the control of the Animal Research Committee in accordance
171 with both the Guidelines on Animal Experiments in Fukushima
172 Medical University, School of Medicine and the Japanese Government
173 Animal Protection and Management Law.

174 2.2.2. Experimental design

175 Three types of experiments were carried out as stated below.

176 (1) Low-dose experiment

177 Rats received intravenous (i.v.) injections through a tail vein at a
178 dose of 20 mg polymeric micelle/kg body weight in 0.5 ml
179 physiological saline per day 5 times on days 0, 1, 3, 5, and 7. The
180 micelle for the injection was formed from (non-biotinylated)
181 PEG-P(Asp(Bzl)). The control rats received the same volume of
182 physiological saline. Body weights of these rats were measured
183 every other day until day 30. Six rats were used for the micelle-
184 injected group, and six other rats were used for the control
185 group. The rats were sacrificed on day 30 under deep ether
186 anesthesia, and the weights of the brain, heart, lungs, liver,
187 spleen, and kidneys were measured. The major organs and
188 tissues (brain, thymus, lymph node, heart, lungs, liver, spleen,
189 gastro-intestines, pancreas, kidneys, adrenal gland, ovary,
190 uterus, muscle, and bone) were removed and were fixed in
191 10% formalin. These samples were processed for hematoxylin
192 and eosin (HE) staining according to the standard method.

193 (2) High dose experiment

194 Rats received i.v. injections of a polymeric micelle at a dose of
195 200 mg polymeric micelle/kg body weight in 0.5 ml physio-
196 logical saline per day 5 times at days 0, 1, 2, 3, and 4 and were
197 sacrificed on day 8. The micelle for injection was formed with
198 (non-biotinylated)PEG-P(Asp(Bzl)). The control rats received
199 the same volume of physiological saline. The body weights of
200 these rats were measured every day until day 7. Six rats were
201 used for the micelle-injected group and the control group, each.
202 Measurements of organ weights and their histological examina-
203 tions were performed in the same manners as those for the
204 low-dose experiment as described above.

205 (3) Histological observation with tumor-bearing rat

206 Rat ascites hepatoma AH109A cells [30], 4×10^6 cells/0.5 ml
207 physiological saline, were inoculated, specifically in the sub-
208 cutaneous tissues of the abdominal walls of 10 rats on day 0.
209 Two rats received i.v. with 10 mg biotinylated micelles
210 dispersed in 1 ml of physiological saline on day 2 and day 3
211 and were sacrificed 1 h and 1 day after the injection, respec-
212 tively. This dose corresponds to approx. 60–80 mg/kg. On day 7,
213 6 rats received i.v. with 10 mg biotinylated micelles in 1 ml
214 physiological saline. Two rats were sacrificed 1 h later, and
215 other two rats were sacrificed 1 day later, and two other rats
216 were sacrificed 1 week later. On day 14, two rats received i.v.
217 with 10 mg biotinylated micelles. One rat was sacrificed 1 h
218 later, and the other one was sacrificed 1 day later. All rats were
219 sacrificed under deep ether anesthesia followed by Nembutal
220 (pentobarbital sodium) anesthesia with circulation of physio-
221 logical saline of 50–100 ml from the left ventricle to the right
222 atrium.

223 2.3. Histology and immunohistochemistry

224 Histological materials were fixed in 10% formalin and embedded in 2
225 paraffin, and then sections with 3 μ m thickness were prepared. These 2
226 thin sections were placed on glass slides, deparaffined in xylene, and 2
227 dehydrated in graded alcohols. These slides were stained with 2
228 hematoxylin and eosin (HE). Immunohistochemistry was performed 2
229 according to a streptavidin–biotin complex method as described 2
230 previously [31]. Briefly, endogenous peroxidase was blocked in 0.3% 2
231 H_2O_2 in 100% methanol for 10 min. Some slides were sonicated for 10 min 2
232 in a citrate buffer, pH 6.0. So that there would be a reduction in the 2
233 nonspecific binding of the primary antibodies, sections were preincu- 2
234 cated for 20 min at room temperature in 2% bovine serum albumin (BSA, 234
235 Sigma, St. Louis, MO, USA). After washing with PBS, slides were covered 235
236 with primary antibodies described below for overnight at 4 °C. Incubation 236
237 with biotinylated secondary antibodies (Nichirei, Tokyo, Japan) was done 237
238 at room temperature for 30 min. We applied a streptavidin–biotin– 238
239 peroxidase complex (Nichirei, Tokyo, Japan or Vector Laboratories, 239
240 Burlingame, CA, USA) to each slide. Binding was detected by hydrogen 240
241 peroxidase/3,3'-diaminobenzidine tetrahydrochloride (DAB, Dojindo, 241
242 Kumamoto, Japan). Hematoxylin was used for counterstaining. Sections 242
243 with known expression of the respective epitope were used as positive 243
244 controls, whereas the primary antibody was replaced with an antibody- 244
245 dilution solution, serving as negative controls.

246 An anti-rat CD68 mouse monoclonal antibody was purchased 246
247 from HyCult biotechnology b.v. (Uden, Netherlands). The antibody of 247
248 1 μ g/100 μ l PBS was applied to every slide. The mouse anti-biotin 248
249 monoclonal antibody was purchased from Roche Diagnostic GmbH 249
250 (Penzberg, Germany). The antibody of 1 μ g/100 μ l PBS was applied to 250
251 every slide.

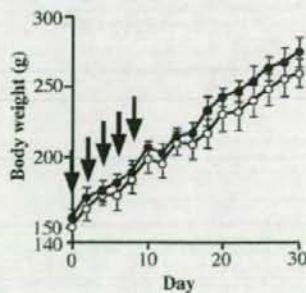
252 2.4. Statistical analysis

253 Data between groups were compared by means of Student's *t*-test. 253
254 Differences were considered to be significant when $p < 0.05$.

255 3. Results

256 3.1. Toxicity examinations

257 In the low-dose experiment (20 mg polymer/kg), the average body 257
258 weight of the micelle-injected group was compared with that of the 258
259 control group. As shown in Fig. 2, there was no statistically significant 259
260 difference in body weights between the two groups although the 260
261 micelle-injected group was slightly lighter than the control prior to 261
262 the first injection. The weights of the brain, heart, lungs, liver, spleen, 262
263 and kidneys of micelle-group rats did not differ from those of the 263
264 control group as summarized in Table 1. No particular pathological 264



259 Fig. 2. Body-weight change in rats that received 20 mg/kg micelle or physiological saline
260 5 times (at arrows). No statistically significant differences were found between the
261 micelle group and the control group.

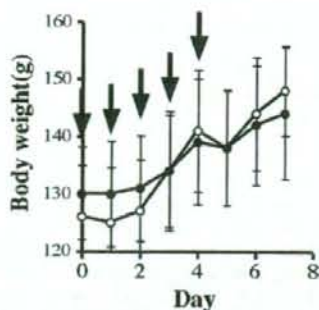


Fig. 3. Body-weight change in rats that received 200 mg/kg micelle or physiological saline 5 times at arrows. No statistically significant differences were found between the micelle group and the control groups.

changes were found in all these examined organs and tissues including bone marrow. Foamy cells were found focally in the lungs and lymph nodes in some rats as shown in Fig. 4a and c, respectively. Foamy-cell accumulation was observed in the lungs and the lymph nodes of the control group, but the degrees were milder than those of the micelle groups as shown in Fig. 4b and d.

Since no toxicity was observed in the low-dose experiment as stated above, a further pathological examination was carried out with an injected dose raised to 200 mg/kg so that there could be an accurate determination of any possible side effect of the micelle. The micelle was intravenously injected at 200 mg polymer/kg 5 times every day into rats, followed by (1) detailed examinations of body weight and organ weight, and (2) histology of organs/tissues. As shown in Fig. 3 and Table 1, there were no differences in the average body weight and in the average organ weight of rats between the micelle-treated group and the control group. In histological observations of HE sections, no abnormality was found in most examined organs and tissues.

One marked change in the micelle-treated group was seen: an increase of foamy cells in the spleen. This increase was observed in all treated rats as shown in Fig. 4e. This finding shows a clear contrast between the spleen of the micelle-injected group (Fig. 4e) and the spleen of the control (Fig. 4f). Staining with the anti-rat CD68 monoclonal antibody confirmed that the foamy cells were macrophages, as shown in Fig. 4g. Immunohistological examinations revealed marked increases in CD68-positive macrophages in the spleen, liver, lymph node, and lungs of the micelle-injected group when these sections were compared with those of the control group (Fig. 4g, i, and k for the rat injected with the micelle and Fig. 4h, j, and l for the control group.). The increase was much more dramatic in the spleen than in the liver and the lungs. The CD-68 immunohistological examination in lymph node was

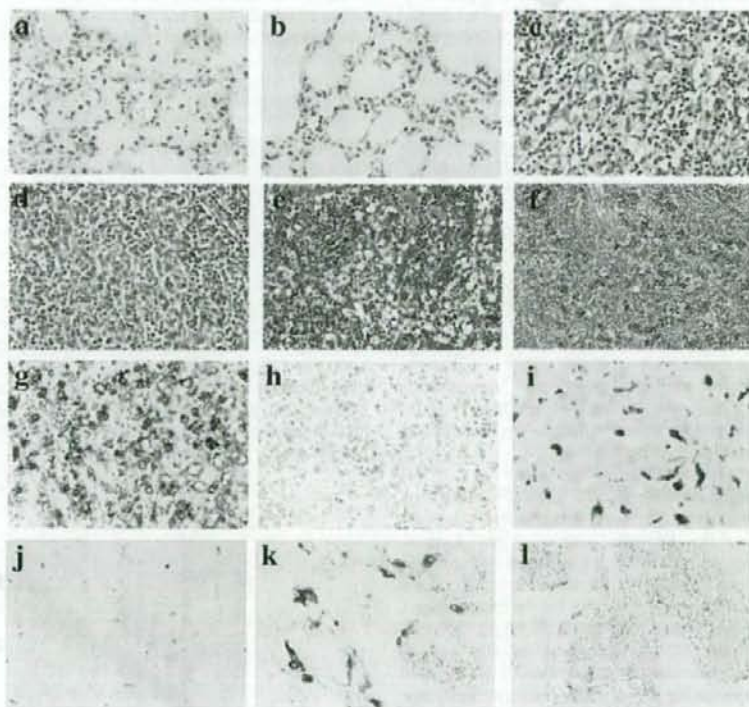


Fig. 4. Histological and immunohistochemical demonstrations of activated MPS in rats that received the micelle. $\times 400$ in the original. (a)–(f): HE staining, and (g)–(l): immunostaining with mouse anti-rat CD68 monoclonal antibody. (a) and (c): accumulation of foamy cells in the lungs and lymph nodes, respectively, belonging to rats that received 20 mg/kg $\times 5$ times and were sacrificed at 30 days after the first injection of the micelle. (b) and (d): lungs and lymph nodes of the control groups, respectively. Foamy-cell accumulation was observed in the lungs and the lymph nodes of the control group, but the degrees were milder than those of the micelle groups. (e): foamy cells in the spleen. Foamy cells were accumulated in the spleens belonging to all rats that received 200 mg/kg $\times 5$ times and were killed at 7 days after the first injection of the micelle. (f): foamy-cell accumulation was rarely found in the spleen of control rats. Here is an immunohistochemical demonstration of activated MPS in (g) the spleen, (i) the liver, and (k) the lungs of the micelle-injected rats. Control mice exhibited smaller numbers of immunostaining-positive cells in (h) the spleen, (j) the liver, and (l) the lungs.

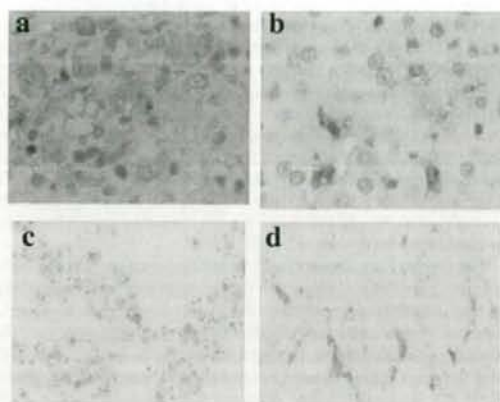


Fig. 5. Immunohistochemistry-based demonstration of biotinylated micelles. Anti-biotin antibody-positive signs were found on mononuclear cells in (a) the spleen, (b) the liver (Kupffer cells), and (c) the lungs (alveolar macrophage). Biotin-positive signs were also found in (d) renal tubules. These tissues were taken from a rat that bore a 2-week-old tumor and that had been sacrificed 24 h after the i.v. injection of 10 mg of biotinylated micelle / rat.

not done. From their intra-sinusoidal location and features, the foamy cells in the liver appeared to be Kupffer cells.

3.2. Microscopic observation of biotinylated micelle disposition with tumor-bearing rats

For immunohistological examinations, a biotinylated micelle was prepared (its chemical structure is shown in Fig. 1) for clarification of the micelle's accumulation behavior in tumor-bearing rats. One hour after the i.v. injection, no sign of the biotinylated micelle accumulation was found in most organs and tissues, including the spleen, liver, lungs, and lymph nodes. In contrast, biotinylated micelle-positive signs were found in the mononuclear phagocyte system (MPS) of the spleen, liver (Kupffer cells), and lungs 1 day after the injection, as shown in Fig. 5a–c. In addition, micelle accumulation was found in intra-tubules of kidneys (Fig. 5d). The biotinylated micelles were detected clearly in the MPS of the liver 1 week after the injection. (data not shown).

Disposition of the biotinylated micelle at the AH109A tumor was observed. As shown in Fig. 6a, the biotinylated micelle accumulation was evident as early as 1 h after injection in the blood vessels of the tumors that were transplanted 2 weeks before the micelle injection. This is a very interesting phenomenon because 1 h is a much shorter period than those are generally argued in targeting of the long-circulating drug carrier systems (e.g., PEG-coated liposomes and polymeric micelles) that utilize the EPR effect as a passive targeting strategy. It was reported that these long-circulating drug carrier systems provided the maximum delivery amounts at the tumor tissues 24 or 48 h post intravenous injection [18,33]. This unique and speedy micelle accumulation was also observed in younger 2-day-old and 1-week-old tumors. (The current study analyzed these tumors 2 days and 1 week after the tumor transplantation.) (data not shown) In enlarged images (Fig. 6b and c), most of the biotin-positive images were found in a highly concentrated manner. As shown in Fig. 6d, an elastic fiber staining image clearly indicates this is an arterial blood vessel.

This finding suggests that the observed micelles were aggregates of the micelles, not dispersed micelles. However, this issue needs further examination for confirmation of the observation in question.

The current study conducted this immunohistological examination both in the peripheral areas and the central areas of the tumor. Fig. 7a and b shows the immunohistological images of the peripheral and central parts, respectively. As shown in Fig. 7a for a 2-week-old tumor-

bearing rat, the micelles were clearly observed in the blood vessels of 3 the tumor capsule 1 day after the micelle injection. The micelles were also 3 observed in the tumor parenchyma (tumor cells, tumor interstitium of 3 blood vessels, and fibrous tissue) The range of tumor parenchyma which 3 showed the micelle-positive signs was approximate 200 μ m, and the 3 micelle-positive signs in the tumor parenchyma showed smaller and 3 finer granular appearance than the micelle-positive signs in the capsular 3 blood vessels. Fig. 7b shows that the micelles were also observed in the 3 dilated and distorted blood vessels of the central tumor area, and that 3 fine granular micelle-positive deposits were found in tumor cells 3 neighboring to these blood vessels. This image was obtained 1 week 3 after the i.v. injection of the micelle. These findings suggest that the 3 observed micelles in the blood vessels were the aggregates of the 346 micelles, while the micelles in the tumor parenchyma were the 347 dispersed micelles. It is commonly accepted that delivery to a tumor's 348 central area is very difficult owing to several inhibitory issues such as 349 high interstitial pressure. In fact, the first paper concerning the EPR effect 350 reported that macromolecules' delivery to the central area was much 351 less effective than the delivery to the peripheral area [7] Therefore, this 352 micelle accumulation in the center area is interesting. The micelles were 353 not clearly observed in extravascular space also in the case where the 354 micelle accumulated in the central area of the tumor. 355

4. Discussion

The polymeric micelle drug carrier system is advantageous for a 357 container of hydrophobic drugs owing to the hydrated micelle outer 358

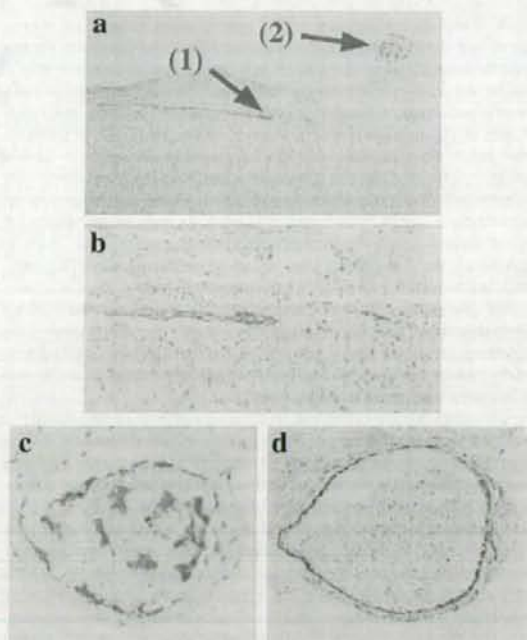


Fig. 6. Tumor targeting of biotinylated micelles. A rat with a 2-week-old tumor was injected with biotinylated micelles and was sacrificed under circulation of 100 ml physiological saline 1 h after the injection. (a) Blood vessels of peri-tumor connective tissues (capsule of tumor) exhibited strong anti-biotin antibody-positive signs. (b) Enlargement of arrow (1). The blood vessel seemed to be a capillary. (c) Enlargement of arrow (2). Anti-biotin antibody-positive signs were found along a blood-vessel surface in addition to a surface of a mass in the blood vessel. Some of the positive signs were seen in the blood. (d) Elastic fiber staining of panel c. This staining indicates that this is an arterial blood vessel.

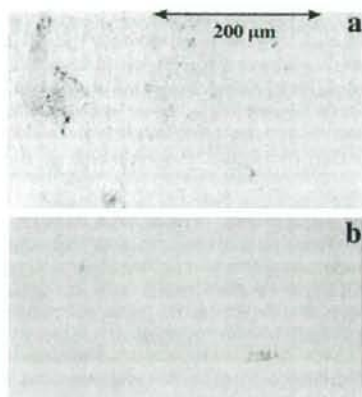


Fig. 7. Immunohistochemical observation of polymeric micelles at different areas of the tumor. (a) The micelles appeared in blood vessels of the tumor peripheral area. The material was taken from a 2-week-old-tumor 1 day after the i.v. injection of biotinylated micelle. The micelles appeared in the blood vessels of the tumor peripheral area (tumor capsule) and tumor parenchyma (tumor cells and tumor blood vessels) near the tumor capsule. (b) The micelles were detected in tumor blood vessels in the center area of the tumor 1 week after the i.v. injection into the 1-week-old-tumor. The micelles were detected in dilated and irregular-shaped blood vessels in center areas of the tumor 1 week after the i.v. injection into the 1-week-old tumor, where necrosis and degeneration occurred. The micelles were also detected in intact tumor cells around such blood vessels.

shell, which can effectively inhibit precipitation caused by hydrophobicity of the incorporated drug. In addition, the block copolymer micelle incorporating anti-cancer drug can accumulate selectively at tumor tissues by means of the EPR effect [7,8,32]. No studies have closely examined biological activities related to possible toxic side effects of the polymeric micelle carriers, although *in vivo* results for anti-cancer drug polymeric micelles suggested no or very low carrier-related toxicities. Concerning the EPR effect's selective accumulation, many reports have supported this EPR effect-based targeting strategy; nevertheless, several fundamental questions remain unelucidated: What parts of tumor tissues and vasculatures are the most active in exhibiting the EPR effect? How quick is permeation of polymeric micelles in tumor interstitium? And how dependent are the above-stated phenomena on the size of polymeric micelles? The authors have developed the PEG-P(Asp(Bzl)) micelle for anti-cancer drug targeting [26,27,29]. Using this PEG-P(Asp(Bzl)) micelle, the present study conducted the first detailed examinations of the acute *in vivo* effects of a polymeric micelle carrier.

The current study detected no toxic side effects of the micelle in any examined organs/tissues, even in cases where there was a large injection dose of the micelles (200 mg/kg \times 5). There was only one marked change in a micelle-treated rat: the activation of the mononuclear phagocyte system (MPS); also, the micelle exhibited a high accumulation in the MPS of the spleen, lungs, lymph node, and liver (Kupffer cells). This study constitutes the first report histologically demonstrating the accumulation of block copolymer micelles in the MPS *in vivo*. This activation is not a pathological change, but may be important to immunological reactions such as the ABC phenomenon [22-25]. Previous research reported that the polymeric micelle carrier system accumulated in the liver at a higher concentration than in other normal organs, and that the accumulated micelle remained present in the liver for a longer time than did a free drug [33]. One related point should be noted: it is evident that the biologically inert property of the PEG outer shell works efficiently to evade the MPS's very rapid micelle uptake, and, consequently, supports the micelle's long-circulation behavior in the bloodstream; however, this evasion was not perfect, providing a certain degree of the MPS uptake. In any

case, because of this accumulation behavior of the micelle at the liver, strong liver toxicity was worrisome, but animal experiments and clinical results of various studies indicated that liver toxicities of the polymeric micelle systems were no more than those of the corresponding free drugs [9,14,15,33]. A possible reason for this mild liver toxicity is that the polymeric micelles accumulate only at liver's Kupffer cells, not at the liver's parenchymal cells (hepatocyte). As reported in our reference [9], the liver toxicities of doxorubicin-containing micelle evaluated with AST and ALT values were found to be milder than free doxorubicin. However, a further study is required for elucidation on this point.

The current study asserts that the MPS was activated in association with its uptake of the polymeric micelle, and that as a result of this activation, the MPS became foamy cells. In relation to the ABC phenomenon, an immunohistological observation was performed for IgM-expressing lymphocytes in the spleen at a high dose (200 mg/kg \times 5). However, no change in the number of IgM-expressing lymphocytes was observed in the spleen (data not shown). At present, the fate of the micelles that accumulated in the MPS cells has not been examined.

Interestingly, the current study found the biotinylated micelles in the blood vessels of tumors' peripheries (capsules) a very short time after the inoculation (1 h) and in the tumors' blood vessels 1 day after the injection. By using HPLC or radioisotope measurements of the accumulated amounts at tumor mass, preceding reports were able to show the tumor-selective accumulation of the polymeric micelles [2,10,16,27,34,35]. In these reports, the polymeric micelles showed the highest tumor accumulation at 24 h post intravenous injection. Thrombus seems at least in parts to be related to this micelle retention in the tumor blood vessels shown in Fig. 7. The EPR effect is known to facilitate the selective accumulation of the micelles at tumors. We observed much stronger micelle image in the blood vessel than in the tumor tissue 1 day after the injection with the immunostaining as shown in Fig. 7a. This observation suggests that the micelle-accumulation mechanism at specific sites of tumors is quicker than the accumulation driven by the EPR effect. However, only further studies can yield rigid evidence about the specific accumulation of micelles in the tumor blood vessels and the tumor tissues, because the research community generally believes that, when immunohistochemistry is the means, detection of dispersed micelles is more difficult to achieve than is detection of aggregates of micelles; and another general belief in the research community is that only dispersed micelles (not aggregated micelles) can be delivered by means of the EPR effect. (As described in the Results section, the micelles were found in tumor vasculatures in a highly concentrated manner, implying that the observed micelles were aggregates of the micelles rather than dispersed micelles.)

5. Conclusion

In this study's detailed histological examination, no pathological abnormality was observed for a systemic injection of PEG-P(Asp(Bzl)) polymeric micelles. The only marked change was activation of the MPS. These results confirmed the high safety of polymeric micelle drug carriers, but suggested the need of further investigation into polymeric micelles' interactions with the MPS. The immunohistochemical analyses also revealed very rapid and specific accumulation of the micelle in the vasculatures of tumor capsule of rat ascites hepatoma AH109A.

Acknowledgments

This work was supported by Grants-in-Aids from the Ministry of Health, Labour and Welfare of Japan. M. Nishihara, T. Yamamoto and M. Yokoyama acknowledge support from the Program for Promoting the Establishment of Strategic Research Centers, Special Coordination Funds for Promoting Science and Technology, and the Ministry of Education, Culture, Sports, Science, and Technology, Japan.

References

- 458
- 459 [1] M. Yokoyama, M. Miyauchi, N. Yamada, T. Okano, Y. Sakurai, K. Kataoka, S. Inoue,
460 Characterization and anticancer activity of the micelle-forming polymeric anticancer
461 drug adriamycin-conjugated poly(ethylene glycol)-poly(aspartic acid) block
462 copolymer, *Cancer Res.* 50 (1990) 1693–1700.
- 463 [2] M. Yokoyama, T. Okano, Y. Sakurai, S. Fukushima, K. Okamoto, K. Kataoka, Selective
464 delivery of adriamycin to a solid tumor using a polymeric micelle carrier system,
465 *J. Drug Target.* 7 (1999) 171–186.
- 466 [3] R. Sevic, A. Eisenberg, D. Maysinger, Block copolymer micelles as delivery vehicles
467 of hydrophobic drugs: micelle-cell interactions, *J. Drug Target.* 14 (2006) 343–355.
- 468 [4] D. Sutton, N. Nasongkla, E. Blanco, J. Gao, Functionalized micelle systems for cancer
469 targeted drug delivery, *Pharm. Res.* 24 (2007) 1029–1046.
- 470 [5] S.C. Kim, D.W. Kim, Y.H. Shim, J.S. Bang, H.S. Oh, S.W. Kim, M.H. Seo, In vivo evaluation
471 of polymeric micellar paclitaxel formulation: toxicity and efficacy, *J. Control. Release*
472 *72* (2001) 191–202.
- 473 [6] T.-Y. Kim, D.-W. Kim, J.-Y. Chung, S.-G. Shin, S.-C. Kim, D.-S. Heo, N.-K. Kim, Y.-J. Bang, Phase
474 I and pharmacokinetic study of Genexol-PM, a cremophor-free, polymeric micelle-
475 formulated paclitaxel, in patients with advanced malignancies, *Clin. Cancer Res.* 10
476 (2004) 3708–3716.
- 477 [7] Y. Matsumura, H. Maeda, A new concept for macromolecular therapeutics in
478 cancer chemotherapy: mechanism of tumorotropic accumulation of proteins and
479 the antitumor agent smancs, *Cancer Res.* 46 (1986) 6387–6392.
- 480 [8] H. Maeda, L.W. Seymour, Y. Miyamoto, Conjugates of anticancer agents and polymers:
481 advantages of macromolecular therapeutics in vivo, *Bioconjug. Chem.* 3 (1992)
482 351–361.
- 483 [9] H. Uchino, Y. Matsumura, T. Negishi, F. Koizumi, T. Hayashi, T. Honda, N. Nishiyama, K.
484 Kataoka, S. Naito, T. Kakizoe, Cisplatin-incorporated polymeric micelle (NC-6004) can
485 reduce nephrotoxicity and neurotoxicity of cisplatin in rats, *Br. J. Cancer* 19 (2005)
486 678–687.
- 487 [10] T. Hamaguchi, Y. Matsumura, M. Suzuki, K. Shimizu, R. Goda, I. Nakamura, I. Nakatomi,
488 M. Yokoyama, K. Kataoka, T. Kakizoe, NK105, a paclitaxel-incorporating micellar
489 nanoparticle formulation, can extend in vivo antitumor activity and reduce the
490 neurotoxicity of paclitaxel, *Br. J. Cancer* 92 (2005) 1240–1246.
- 491 [11] H. Uchino, Y. Matsumura, T. Negishi, F. Koizumi, T. Hayashi, T. Honda, N. Nishiyama, K.
492 Kataoka, S. Naito, T. Kakizoe, Cisplatin-incorporated polymeric micelle (NC-6004) can
493 reduce nephrotoxicity and neurotoxicity of cisplatin in rats, *Br. J. Cancer* 19 (2005)
494 678–687.
- 495 [12] Y. Mizumura, Y. Matsumura, M. Yokoyama, T. Okano, T. Kawaguchi, F. Moriyasu,
496 T. Kakizoe, Incorporation of the anticancer agent KRN5500 into polymeric
497 micelles diminishes the pulmonary toxicity, *Jpn. J. Cancer Res.* 93 (2002) 1273–
498 1243.
- 499 [13] T. Negishi, F. Koizumi, H. Uchino, J. Kuroda, T. Kawaguchi, S. Naito, Y. Matsumura,
500 NK105, a paclitaxel-incorporating micellar nanoparticle, is a more potent radio-
501 sensitizing agent compared to free paclitaxel, *Br. J. Cancer* 95 (2006) 601–606.
- 502 [14] Y. Matsumura, T. Hamaguchi, T. Ura, K. Muro, Y. Yamada, Y. Shimada, K. Shirao, T.
503 Otsuka, H. Ueno, M. Ikeda, N. Watanabe, Phase I clinical trial and pharmacokinetic
504 evaluation of NK911, a micelle-encapsulated doxorubicin, *Br. J. Cancer* 91 (2004)
505 1775–1781.
- 506 [15] T. Hamaguchi, K. Kato, H. Yasui, C. Morizane, M. Ikeda, H. Ueno, K. Muro, Y. Yamada,
507 T. Okusaka, K. Shirao, Y. Shimada, H. Nakahama, Y. Matsumura, A phase I and
508 pharmacokinetic study of NK105, a paclitaxel-incorporating micellar nanoparticle
509 formulation, *Br. J. Cancer* 97 (2007) 170–176.
- 510 [16] F. Koizumi, M. Kitagawa, T. Negishi, T. Onda, S. Matsumoto, T. Hamaguchi, Y. Matsumura,
511 Novel SN-38-incorporating polymeric micelles, NK012, eradicate vascular endothelial
512 growth factor-secreting bulky tumors, *Cancer Res.* 66 (2006) 10048–10056.
- 517 [17] M. Sumitomo, F. Koizumi, T. Asano, A. Horiguchi, K. Ito, T. Asano, T. Kakizoe, M. S.
518 Hayakawa, Y. Matsumura, Novel SN-38-incorporated polymeric micelle, NK012,
519 strongly suppresses renal cancer progression, *Cancer Res.* 68 (2008) 1631–1635.
- 520 [18] D.C. Drummond, D. Kirpotin, C. Benz, J.W. Park, K. Hong, Liposomal drug delivery
521 systems for cancer therapy, in: D.M. Brown (Ed.), *Drug Delivery Systems in Cancer*
522 *Therapy*, Humana Press Inc., Totowa, 2004, pp. 191–213.
- 523 [19] P.R. Hamann, M.S. Berger, Mylotarg: the first antibody-targeted chemotherapy
524 agent, in: M. Page (Ed.), *Tumor Targeting in Cancer Therapy*, Humana Press Inc.,
525 Totowa, 2002, pp. 239–254.
- 526 [20] A.V. Kabanov, J. Zhu, Luronic block copolymers for drug and gene delivery, in: G.S.
527 Kwon (Ed.), *Polymeric Drug Delivery Systems*, Taylor & Francis, Boca Raton, 2005,
528 pp. 577–613.
- 529 [21] E.V. Batrakov, S. Li, W.F. Elmquist, D.W. Miller, V.Y. Alakhov, A.V. Kabanov,
530 Mechanism of sensitization of MDR cancer cells by Pluronic block copolymers:
531 selective energy depletion, *Br. J. Cancer* 85 (2001) 1987–1997.
- 532 [22] E.T.M. Dams, P. Lawverman, W.J.G. Oyen, G. Strom, G.L. Scherphof, J.W.M. van der Meer,
533 F.H.M. Coretns, O.C. Boerman, Accelerated blood clearance and altered biodistribu-
534 tion of repeated injections of sterically stabilized liposomes, *J. Pharmacol. Exp. Ther.*
535 *292* (2000) 1071–1079.
- 536 [23] T. Ishida, M. Ichihara, X. Wang, K. Yamamoto, J. Kimura, E. Majima, H. Kiwada,
537 Injection of PEGylated liposomes in rats elicits PEG-specific IgM, which is responsible
538 for rapid elimination of a second dose of PEGylated liposomes, *J. Control Release* 112
539 (2006) 15–25.
- 540 [24] T. Ishida, H. Kiwada, Accelerated blood clearance (ABC) phenomenon upon
541 repeated injection of PEGylated liposomes, *Int. J. Pharm.* 345 (2008) 56–62.
- 542 [25] H. Koide, T. Asai, K. Hatanaka, T. Urakami, T. Ishii, E. Kenjo, M. Nishihara, M. Yokoyama,
543 T. Ishida, H. Kiwada, and N. Oku, The particle size-dependent occurrence of accelerated
544 blood clearance phenomenon, *Int. J. Pharm.*, in press.
- 545 [26] M. Watanabe, K. Kawano, M. Yokoyama, P. Opanasopit, T. Okano, Y. Maitani,
546 Preparation of camptothecin-loaded polymeric micelles and evaluation of their
547 incorporation and circulation stability, *Int. J. Pharm.* 308 (2006) 183–189.
- 548 [27] K. Kawano, M. Watanabe, T. Yamamoto, M. Yokoyama, P. Opanasopit, T. Okano, Y.
549 Maitani, Enhanced antitumor effect of camptothecin loaded in long-circulating
550 polymeric micelles, *J. Control Release* 112 (2006) 329–332.
- 551 [28] N. Chansri, S. Kawakami, M. Yokoyama, T. Yamamoto, P. Charoensit, M. Hashida,
552 Anti-tumor effect of all-*trans* retinoic acid loaded polymeric micelles in solid
553 tumor bearing mice, *Pharm. Res.* 25 (2008) 428–434.
- 554 [29] M. Yokoyama, P. Opanasopit, Y. Maitani, K. Kawano, T. Okano, Polymer design and
555 incorporation method for polymeric micelle carrier system containing water-
556 insoluble anti-cancer agent camptothecin, *J. Drug Target.* 12 (2004) 373–384.
- 557 [30] T. Kawaguchi, S. Imai, S. Haga, J. Morimoto, T. Honda, in: K. Watanabe (Ed.), *Cancer*
558 *Metastases Research*, Nova Science Publisher, 2008, pp. 147–163.
- 559 [31] S.M. Hue, L. Raine, H. Fanger, Use of avidin-biotin-peroxidase complex (ABC) in
560 immunoperoxidase techniques: a comparison between ABC and unlabeled anti-
561 body (PAP) procedures, *J. Histochem. Cytochem.* 29 (1981) 577–580.
- 562 [32] F.M. Muggia, Doxorubicin-polymer conjugates: further demonstration of the
563 concept of enhanced permeability and retention, *Clin. Cancer Res.* 5 (1999) 7–8.
- 564 [33] M. Yokoyama, T. Okano, Y. Sakurai, H. Ekimoto, C. Shibasaki, K. Kataoka, Toxicity and
565 antitumor activity against solid tumors of micelle-forming polymeric anticancer
566 drug and its extremely long circulation in blood, *Cancer Res.* 51 (1991) 3229–3236.
- 567 [34] G.S. Kwon, S. Suwa, M. Yokoyama, T. Okano, Y. Sakurai, K. Kataoka, Enhanced tumor
568 accumulation and prolonged circulation times of micelle-forming poly(ethylene oxide-
569 aspartate) block copolymer-adriamycin conjugates, *J. Control Release* 29 (1994) 17–23.
- 570 [35] N. Nishiyama, S. Okazaki, H. Cabral, M. Miyamoto, Y. Kato, Y. Sugiyama, K. Nishio, Y.
571 Matsumura, K. Kataoka, Novel cisplatin-incorporated polymeric micelles can eradicate
572 solid tumors in mice, *Cancer Res.* 63 (2003) 8977–8983.
- 573
- 574
- 575
- 576
- 577
- 578
- 579
- 580
- 581
- 582
- 583
- 584
- 585
- 586
- 587
- 588
- 589
- 590
- 591
- 592
- 593
- 594
- 595
- 596
- 597
- 598
- 599
- 600



Pharmaceutical nanotechnology

Enhanced *in vivo* antitumor efficacy of fenretinide encapsulated in polymeric micellesTomoyuki Okuda^a, Shigeru Kawakami^a, Yuriko Higuchi^a, Taku Satoh^b, Yoshimi Oka^b, Masayuki Yokoyama^b, Fumiyoshi Yamashita^a, Mitsuru Hashida^{a,c,*}^a Department of Drug Delivery Research, Graduate School of Pharmaceutical Sciences, Kyoto University, Sakyo-ku, Kyoto 606-8501, Japan^b Kanagawa Academy of Science and Technology, KSP East 404, Sakado 3-2-1, Takatsu-ku, Kawasaki-shi, Kanagawa 213-0012, Japan^c Institute of Integrated Cell-Material Sciences (iCeMS), Kyoto University, Yoshida, Sakyo-ku, Kyoto 606-8501, Japan

ARTICLE INFO

Article history:

Received 3 October 2008

Received in revised form 21 January 2009

Accepted 23 January 2009

Available online xxx

Keywords:

Fenretinide

4-HPR

Retinoid

Polymeric micelle

Controlled release

Drug delivery system

ABSTRACT

Fenretinide (N-(4-hydroxyphenyl)retinamide, 4-HPR) is a synthetic retinoid with high antitumor activity against a variety of malignant cells *in vitro*, and is a promising candidate for cancer chemoprevention and chemotherapy. To enhance the antitumor efficacy of 4-HPR *in vivo*, 4-HPR were encapsulated into polymeric micelles for tumor targeting by enhanced permeability and retention effects. 4-HPR encapsulated in poly(ethylene glycol)-poly(benzyl aspartate) block copolymer micelles were prepared by the evaporation method. The mean particle size of 4-HPR encapsulated in polymeric micelles was about 173 nm. After intravenous injection into tumor-bearing mice, the delivery of 4-HPR by polymeric micelles increased the blood concentration and enhanced the tumor accumulation of 4-HPR over the injection of the 4-HPR encapsulated in oil-in-water (O/W) emulsions. Tumor growth was significantly delayed following treatment by 4-HPR encapsulated in polymeric micelles, which demonstrated the improved *in vivo* antitumor efficacy of 4-HPR. In addition, 4-HPR encapsulated in polymeric micelles did not cause any body weight loss. These results suggest that polymeric micelles are a promising and effective carrier of 4-HPR in order to enhance tumor delivery and have potential application in the treatment of solid tumor.

© 2009 Published by Elsevier B.V.

1. Introduction

Retinoids are a class of natural or synthetic derivatives of vitamin A that exert various biological actions on cellular growth and differentiation (Means and Gudas, 1995; Kagechika and Shudo, 2005). As a result of their unique characteristics, their application in novel cancer therapy has been progressing (Altucci and Gronemeyer, 2001; Clarke et al., 2004). In particular, fenretinide (N-(4-hydroxyphenyl)retinamide, 4-HPR), which was synthesized from all-trans retinoic acid (ATRA), is a promising candidate for cancer chemoprevention and chemotherapy, since it has higher antitumor activity and lower toxicity than other retinoids (Moon et al., 1979; Miller, 1998). It was reported that the antitumor activity of 4-HPR was through two main mechanisms: retinoic acid receptor-dependent cascade and retinoic acid receptor-independent cascade, including reactive oxygen species generation, ceramide synthesis, and proapoptotic bcl-2 family protein (Bax and

Bak) induction (Hail et al., 2006; Corazzari et al., 2005). Clinical trials of 4-HPR have been progressing against breast cancer, prostate cancer, and neuroblastoma (Altucci and Gronemeyer, 2001; Clarke et al., 2004).

To date, 4-HPR has been clinically administered using an oral gelatin capsule containing 4-HPR in corn oil and polysorbate 80 [available through the National Cancer Institute]; however, this formulation has poor bioavailability, since 4-HPR itself is too hydrophobic to pass through intestinal membrane easily (Kokate et al., 2007), and requires excessive or multiple administrations to achieve a higher blood concentration of 4-HPR (Villablanca et al., 2006). In addition, several animal studies have demonstrated that intravenously injected 4-HPR is rapidly eliminated from the body (Swanson et al., 1980; Hultin et al., 1986); therefore, the development of a targeted carrier of 4-HPR is needed to exert *in vivo* antitumor efficacy.

Polymeric micelles are a class of micelles that are formed from block copolymers typically consisting of hydrophilic and hydrophobic polymer chains (Kataoka et al., 2001; Torchilin, 2004). They are of particular interest because of their efficacy in entrapping a satisfactory amount of hydrophobic drugs within the inner core, their stability in the circulation and their ability to gradually release the drugs (Kwon, 2003). In addition, the highly hydrated outer

* Corresponding author at: Department of Drug Delivery Research, Graduate School of Pharmaceutical Sciences, Kyoto University, Sakyo-ku, Kyoto 606-8501, Japan. Tel.: +81 75 753 4525; fax: +81 75 753 4575.

E-mail address: hashidam@pharm.kyoto-u.ac.jp (M. Hashida).

shells of the micelles prevent reticuloendothelial system (RES) uptake and inhibit intermicellar aggregation of their hydrophobic inner cores. The characteristics of these polymeric micelles could be an advantage for passive delivery and to extravasate the drug at tumor sites by enhanced permeability and retention (EPR) effects (Maeda, 2001). In our previous report, we demonstrated that poly(ethylene glycol)-poly(aspartate) block copolymer micelles modified with benzyl groups could stably encapsulate 4-HPR and enhanced blood retention of 4-HPR after intravenous injection into mice (Okuda et al., 2008). This observation prompted us to investigate the potential use of polymeric micelles to enhance tumor retention and *in vivo* antitumor efficacy of 4-HPR in tumor-bearing mice.

In this study, we extended our previous study and tumor distribution and antitumor efficacy of 4-HPR encapsulated in poly(ethylene glycol)-poly(aspartate) block copolymer micelles modified with benzyl groups after intravenous injection were examined in mice bearing murine melanoma B16BL6 tumors. As a control pharmaceutical formulation of 4-HPR, oil-in-water (O/W) or PEGylated O/W emulsions were selected because of their preparation characteristics for delivery of highly lipophilic drugs (Tamilvanan, 2004).

2. Materials and methods

2.1. Materials

4-HPR was purchased from Tokyo Chemical Industry, Co. Ltd. (Tokyo, Japan). Egg yolk phosphatidylcholine (EggPC) and 3-(4,5-dimethyl-2-thiazoyl)-2,5-diphenyl-2H tetrazolium bromide (MTT) were purchased from Sigma-Aldrich (St. Louis, MO, USA). Soybean oil (SO) and ATRA were purchased from Wako Pure Chemicals Industry, Ltd. (Osaka, Japan). Acetonitrile (HPLC grade) and acetic acid (HPLC grade) were purchased from Nacalai Tesque, Inc. (Kyoto, Japan). Distearoylphosphatidylethanolamine-N-[methoxy(polyethylene glycol)-2000] (PEG-DSPE) was purchased from Nippon Oil and Fats Co. (Tokyo, Japan). Fetal bovine serum (FBS) was obtained from Biowhittaker (Walkersville, MD). Dulbecco's modified Eagle's medium (DMEM), phosphate-buffered saline (PBS), and Hank's balanced saline solution (HBSS) were purchased from Nissui Pharmaceutical Co., Ltd. (Tokyo, Japan). All other chemicals were of the highest purity available.

2.2. Synthesis of block copolymer

Poly(ethylene glycol)-poly(aspartic acid) (PEG-P(Asp)) block copolymer was obtained by alkaline hydrolysis of poly(ethylene glycol)-poly(β -benzyl-L-aspartate) (PEG-PBLA), as reported previously (Opanasopit et al., 2004). Briefly, the molecular weight of poly(ethylene glycol) (PEG) chain was 5000 and the average number of aspartic acid units was 27. Approximately 75% of the aspartic acid residues in poly(aspartic acid) chain were converted to the β -amide form by alkaline hydrolysis during the synthesis of this block copolymer. A hydrophobic benzyl group was bound to 77% of the poly(aspartic acid) residues by an ester-forming reaction between benzyl bromide and PEG-P(Asp), as reported previously (Yokoyama et al., 2004). Briefly, PEG-P(Asp) block copolymer was dissolved in N,N-dimethylformamide (DMF) and added to benzyl bromide along with a catalyst, 1,8-diazabicyclo[5.4.0]7-undecene (DBU). The reaction mixture was stirred at 50 °C for 15.5 h. Polymer was obtained by precipitation in excess of diethyl ether and collected by filtration. The dried polymer was dissolved in dimethyl sulfoxide (DMSO), and then 6N HCl was added, followed by dialysis against distilled water and finally, freeze-drying.

For determination of the polymer composition, such as the number of aspartic acid units and the benzyl ester content, ^1H NMR

measurements were carried out on a 1% solution in 6D-DMSO containing 3% trifluoroacetic acid using a Varian Unity Inova NMR spectrometer at 400 MHz.

2.3. Preparation of 4-HPR encapsulated in polymeric micelles

4-HPR encapsulated in polymeric micelles was prepared by a conventional evaporation method (Kawakami et al., 2005; Chansri et al., 2008). Briefly, 4-HPR and polymer were dissolved in chloroform. After vacuum drying and desiccation, PBS (pH 7.4) was added for suspension in a bath sonicator for 3 min. The suspension was sonicated for 3 min (200 W) at 75 °C using a probe sonicator (US 300, Nissei, Inc., Tokyo, Japan). The preparation was centrifuged at 1400 \times g for 10 min before the supernatant was passed through a 0.45 μm filter.

2.4. Preparation of 4-HPR encapsulated in O/W emulsions and PEGylated O/W emulsions

4-HPR encapsulated in O/W emulsions was prepared based on our previous reports (Takino et al., 1994; Chansri et al., 2006). Briefly, 4-HPR, EggPC, and SO (30:150:150, weight ratio) were dissolved in chloroform. After vacuum drying and desiccation, PBS (pH 7.4) was added for suspension in a bath sonicator for 3 min. The suspension was sonicated for 30 min (200 W) at 4 °C using a probe sonicator (US 300, Nissei, Inc., Tokyo, Japan). 4-HPR encapsulated in PEGylated O/W emulsions, composed of 4-HPR, EggPC, PEG-DSPE, and SO (30:105:45:150, weight ratio), was also prepared using this protocol.

2.5. Characterization of the formulations

The concentration of 4-HPR in the preparations was determined by UV absorption at 370 nm (UV-vis Spectrophotometer, Shimadzu Co. Ltd., Kyoto, Japan) after dissolving in DMSO (the preparations: DMSO = 10:990, volume ratio). The recovery of 4-HPR was calculated from the concentration of 4-HPR in the preparations (C_p) as follows:

$$\text{Recovery(\%)} = \frac{C_p(\text{mg/mL}) \times \text{added PBS}(\text{mL})}{\text{initial amount of 4-HPR}(\text{mg})} \times 100$$

On the other hand, the recovery of polymer was defined as 100% because of high solubility of polymer in PBS (>50 g/L). The particle sizes and polydispersion indexes of the preparations were measured by Zetasizer Nano Series (Malvern Instruments Ltd., Worcestershire, UK).

2.6. Animals

Male C57BL/6 mice (4 weeks old, 14–19 g) were purchased from the Shizuoka Agricultural Cooperative Association for Laboratory Animals (Shizuoka, Japan). Animals were maintained under conventional housing conditions. All animal experiments were carried out in accordance with the guidelines for Animal Experiments of Kyoto University.

2.7. Tumor cells

Murine melanoma B16BL6 cells were obtained from the Cancer Chemotherapy Center of the Japanese Foundation for Cancer Research (Tokyo, Japan). They were grown in DMEM supplemented with 10% heat-inactivated FBS, 0.15% NaHCO_3 , 100 units/mL penicillin, and 100 $\mu\text{g/mL}$ streptomycin at 37 °C in humidified air containing 5% CO_2 .

2.8. MTT assay

MTT assay was performed by the method described previously (Kawakami et al., 2006). B16BL6 cells were placed on a 96-well cluster dish at a density of 3×10^3 cells/0.28 cm². Twenty-four hours later, medium containing various concentrations of 4-HPR, empty polymeric micelles, and 4-HPR encapsulated in polymeric micelles was added to the plates. At each exposure time point, the medium was removed and 5 mg/mL MTT solution was added to each well. Cells were incubated for 4 h at 37 °C in 5% CO₂ and then 10% sodium dodecyl sulfate (SDS) solution was added, followed by incubation overnight to dissolve formazan crystals. An absorbance was measured at wavelengths of 570 nm in a microplate photometer (Bio-Rad Model 550, Bio-Rad Laboratories, Inc., Hercules, CA, USA). IC₅₀ values were determined from dose-response curves by a nonlinear regression analysis using MULTI program developed by Yamaoka et al. (Yamaoka et al., 1981) and represent the concentration required to inhibit cell viability by 50%.

2.9. Tumor-bearing mouse model

After harvesting by trypsin, B16BL6 cells were prepared at a concentration of 4×10^6 cells/mL by HBSS. Then, 0.05 mL of the cell suspension (2×10^5 cells) was inoculated subcutaneously in the lower back of each C57BL/6 mouse. A solid tumor was observed within 7 days after tumor inoculation.

2.10. In vivo distribution study

4-HPR encapsulated in polymeric micelles, O/W emulsions, and PEGylated O/W emulsions were adjusted to 7.5 mg/mL as 4-HPR. On 14 days after tumor inoculation, they were intravenously injected into the tail vein of B16BL6-bearing mice at a dose of 75 mg/kg as 4-HPR. At each collection time point, blood was collected from the vena cava under anesthesia, and mice were killed for tumor excision. Blood was centrifuged at $5000 \times g$ for 5 min at 4 °C before 200 μ L of plasma was collected. The plasma was added to 400 μ L of acetonitrile and 4 μ L of 2 mg/mL ATRA (dissolved in ethanol) as an internal standard and vortexed. Part 0.2 g of the excised tumor was collected and added to 500 μ L of acetonitrile and 5 μ L of 2 mg/mL ATRA, followed by sonication using a bath sonicator for 15 min. The extract from plasma and tumor was centrifuged at $13,000 \times g$ for 3 min at 4 °C, and the supernatant was collected and passed through a 0.45 μ m filter. The filtrated extract was analyzed by HPLC.

2.11. HPLC conditions

The extract was analyzed with a high-performance liquid chromatograph device, consisting of a system controller (SLC-10A VP, Shimadzu Co. Ltd., Kyoto, Japan), a UV-vis detector (SPD-10A VP, Shimadzu Co. Ltd., Kyoto, Japan), an auto injector (SIL-10A, Shimadzu Co. Ltd., Kyoto, Japan), and a HPLC pump (LC-10AS, Shimadzu Co. Ltd., Kyoto, Japan). The UV-vis detector was set at 350 nm. A C18 reverse-phase column (ODS-A 150 mm \times 4.6 mm, YMC Co. Ltd., Kyoto, Japan) was used. The mobile phase consisted of acetonitrile:water:acetic acid (80:19:1, volume ratio) delivered at a flow rate of 1 mL/min. The injection volume was 50 μ L. All samples were analyzed at room temperature.

2.12. Pharmacokinetic analysis

Pharmacokinetic parameters including the half-life ($t_{1/2}$), the area under the concentration versus time curve ($AUC_{0-\infty}$), the total body clearance (CL_{tot}), the volume of distribution at steady state (V_{dss}), and the mean residence time (MRT) were all calculated by moment analysis program developed by Yamaoka et al. (1978).

2.13. In vivo antitumor efficacy in tumor-bearing mice

On 8 days after tumor inoculation when the tumor volume reached approximately 100 mm³, each treatment was started. 4-HPR encapsulated in polymeric micelles and O/W emulsions was intravenously injected into the tail vein of B16BL6-bearing mice at a dose of 75 mg/(kg day) as 4-HPR. The dose of empty polymeric micelles was 375 mg/(kg day) as polymer, which was an equivalent dose to 4-HPR encapsulated in polymeric micelles. In the control groups, PBS was administered. Each treatment was performed at 10 mL/(kg day) on 8, 10, and 12 days after tumor inoculation. Tumor diameter and body weight were measured for each mouse at 2-day intervals after the treatment started. Tumor volume was calculated as follows:

$$\text{Tumor volume} = \frac{\pi}{6} \times LW^2$$

where L is the long diameter and W is the short diameter.

2.14. Statistical analysis

Statistical comparison was performed by Student's t -test for two groups, and Dunnett's test for multiple groups. $P < 0.05$ was considered significant.

3. Results

3.1. Characteristics of 4-HPR encapsulated in polymeric micelles

Poly(ethylene glycol)-poly(benzyl aspartate) block copolymer was successfully synthesized from PEG-P(Asp), and about 77% of the aspartic residues were esterified with benzyl groups as reported previously (Opanasopit et al., 2004). The recovery of 4-HPR achieved approximately 70% in polymer/4-HPR weight ratio at 2.5 and 3.0 (Fig. 1). Therefore, polymer/4-HPR weight ratio was fixed at 2.5 in the following experiments. The mean particle size of polymeric micelles was about 173 nm (Fig. 2). On the other hand, the mean particle sizes of O/W emulsions and PEGylated O/W emulsions were about 176 and 178 nm, respectively, similar to polymeric micelles. The polydispersion indexes of polymeric micelles, O/W

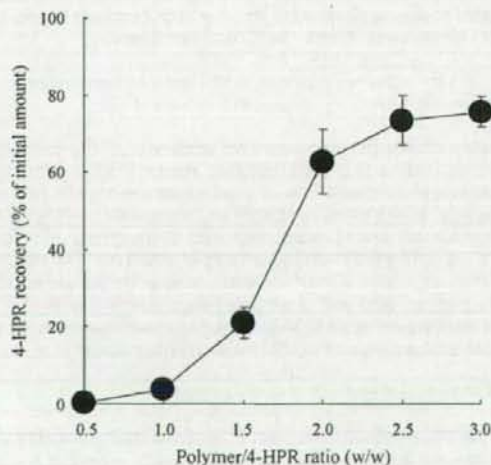


Fig. 1. Effect of polymer/4-HPR weight ratio on encapsulation of 4-HPR into prepared polymeric micelles. 4-HPR encapsulated in polymeric micelles was prepared at various weight ratio for 1 mg 4-HPR, and 4-HPR recovery was calculated. Each value represents the mean \pm S.D. ($n=4$).

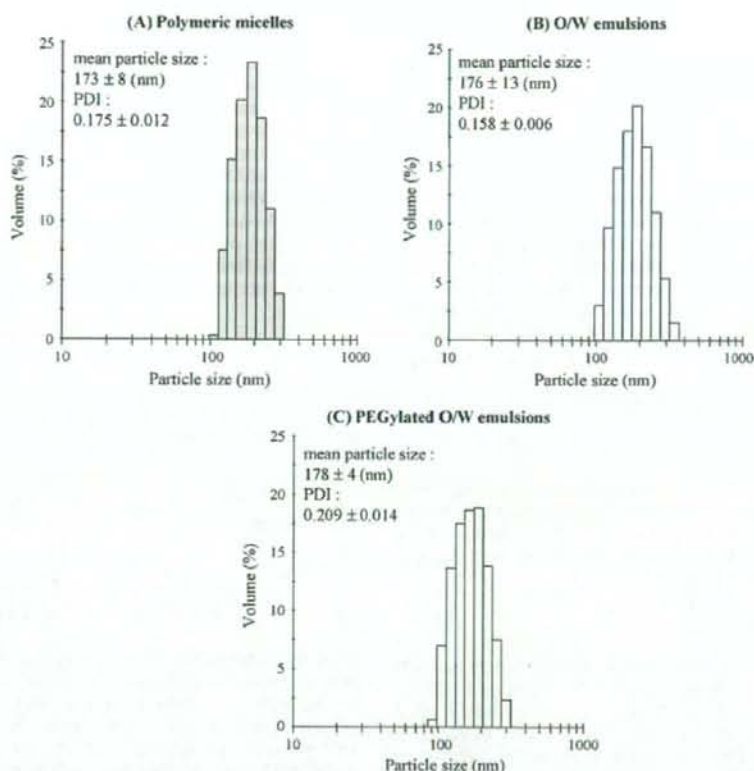


Fig. 2. Size distributions, mean particle sizes, and polydispersion indexes (PDI) of 4-HPR encapsulated in polymeric micelles (A), 4-HPR encapsulated in O/W emulsions (B), and 4-HPR encapsulated in PEGylated O/W emulsions (C). Each value of represents the mean \pm S.D. ($n=3$).

emulsions, and PEGylated O/W emulsions were about 0.175, 0.158, and 0.209, respectively, suggesting the narrow size distribution of these preparations. Furthermore, the particle size of 4-HPR encapsulated in polymeric micelles remained constant over 1 month at room temperature, 4, and -30°C (data not shown).

3.2. *In vitro* antitumor activity of 4-HPR and 4-HPR encapsulated in polymeric micelles

For evaluating *in vitro* antitumor activity of 4-HPR and 4-HPR encapsulated in polymeric micelles against B16BL6 cells, MTT assay was performed. The *in vitro* antitumor activity of 4-HPR was enhanced as the increase of dose and exposure time (Fig. 3(A)). IC_{50} value was settled on approximately $0.60\ \mu\text{g}/\text{mL}$ at more than 24 h, suggesting full antitumor activity of 4-HPR could be obtained at 24 h. IC_{50} value of 4-HPR encapsulated in polymeric micelles ($52\ \mu\text{g}/\text{mL}$ at 48 h) was much larger than that of free form of 4-HPR ($0.60\ \mu\text{g}/\text{mL}$ at 48 h) (Fig. 3(B)). This result may indicate the stable encapsulation of 4-HPR into polymeric micelles in medium.

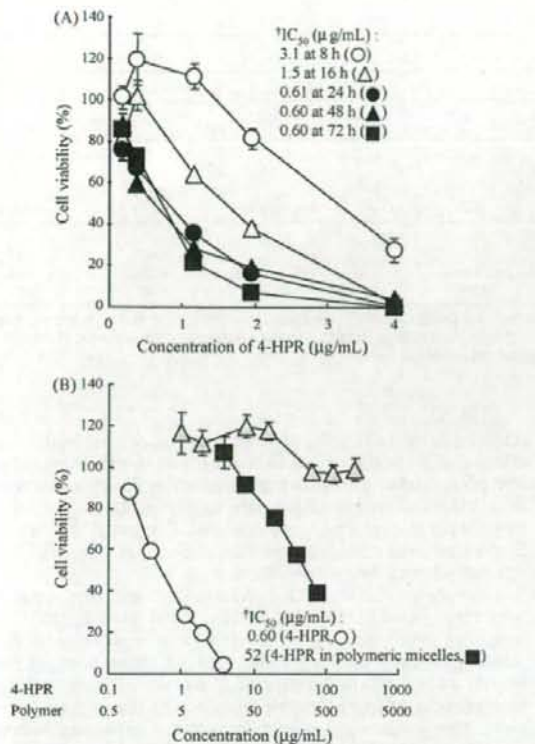
3.3. Distribution of 4-HPR in tumor-bearing mice

The blood concentration and tumor accumulation of 4-HPR after intravenous injection of 4-HPR encapsulated in polymeric micelles were evaluated in B16BL6-bearing mice (Fig. 4) and compared with those of 4-HPR encapsulated in O/W emulsions or PEGylated O/W emulsions as control. The blood concentration of 4-HPR encapsulated in polymeric micelles was significantly higher than

those of 4-HPR encapsulated in O/W emulsions and PEGylated O/W emulsions, suggesting that polymeric micelles could enhance the blood retention of 4-HPR compared with O/W emulsions and PEGylated O/W emulsions. Moreover, the tumor accumulation of 4-HPR encapsulated in polymeric micelles was significantly higher and prolonged for 48 h compared with O/W emulsions and PEGylated O/W emulsions. Pharmacokinetic parameters of 4-HPR encapsulated in polymeric micelles, O/W emulsions, and PEGylated O/W emulsions were shown in Table 1. The area under the curve ($\text{AUC}_{0-\infty}$) in blood was approximately 23.9 times higher for 4-HPR encapsulated in polymeric micelles than for that in O/W emulsions. The $t_{1/2}$ in blood was approximately 5.02 times longer for 4-HPR encapsulated in polymeric micelles than for that in O/W emulsions. Furthermore, the maximum concentration (C_{max}), and the $\text{AUC}_{0-\infty}$ in tumors were approximately 3.03 and 16.9 times higher for 4-HPR encapsulated in polymeric micelles than for that in O/W emulsions, respectively. The $t_{1/2}$ in tumors was approximately 5.63 times longer for 4-HPR encapsulated in polymeric micelles than for that in O/W emulsions.

3.4. *In vivo* antitumor efficacy of 4-HPR encapsulated in polymeric micelles in tumor-bearing mice

In vivo antitumor efficacy of 4-HPR encapsulated in polymeric micelles was evaluated in B16BL6-bearing mice after intravenous injection of PBS (control), empty polymeric micelles, 4-HPR encapsulated in O/W emulsions, and 4-HPR encapsulated in polymeric micelles. Each treatment was performed on 8, 10, and 12 days (total



IC_{50} values were determined from dose-response curves by a nonlinear regression analysis using MULTI program developed by Yamaoka et al. (Yamaoka et al., 1981) and represent the concentration required to inhibit cell viability by 50%.

Fig. 3. *In vitro* antitumor activity of 4-HPR and 4-HPR encapsulated in polymeric micelles against B16BL6 cells. (A) Time and concentration dependence of *in vitro* antitumor activity of 4-HPR. Cell viability was measured by MTT method at 8 h (open circle), 16 h (open triangle), 24 h (filled circle), 48 h (filled triangle), and 72 h (filled square) after treatment. (B) *In vitro* antitumor activity of 4-HPR (open circle), empty polymeric micelles (shaded triangle), and 4-HPR encapsulated in polymeric micelles (filled square) at 48 h after treatment. Each value represents the mean \pm S.D. ($n=3-4$).

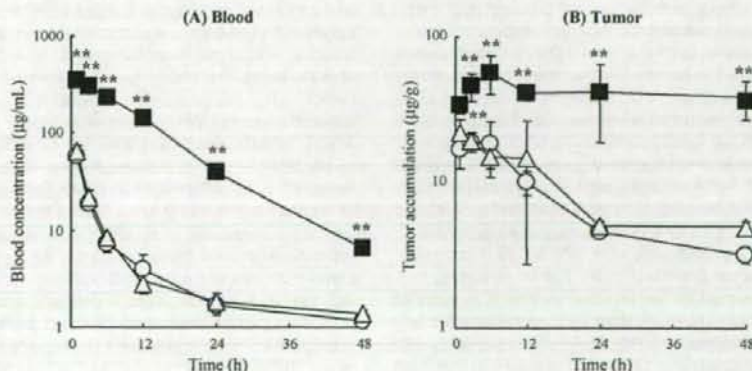


Fig. 4. Blood concentration (A) and tumor accumulation (B) of 4-HPR following intravenous injection of 4-HPR encapsulated in O/W emulsions (open circle), 4-HPR encapsulated in PEGylated O/W emulsions (open triangle), and 4-HPR encapsulated in polymeric micelles (filled square), into B16BL6-bearing mice. Each formulation was intravenously injected at 75 mg/kg dose of 4-HPR on 14 days after tumor inoculation. At indicated time point, blood and tumor were collected and amount of 4-HPR was measured by HPLC. Each value represents the mean \pm S.D. ($n=3-6$). Statistically significant differences compared with 4-HPR encapsulated in O/W emulsions (** $P < 0.01$).

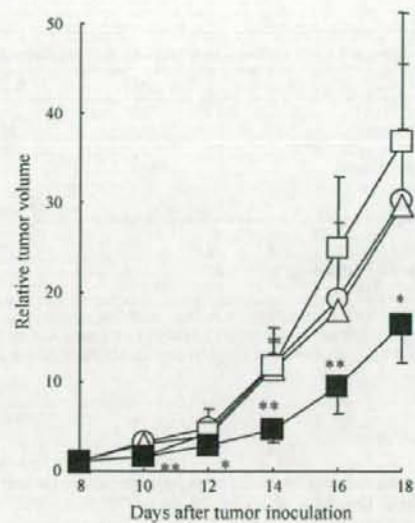


Fig. 5. Relative tumor volume of B16BL6-bearing mice after intravenous injection of PBS (open circle), empty polymeric micelles (open triangle), 4-HPR encapsulated in O/W emulsions (open square), and 4-HPR encapsulated in polymeric micelles (filled square). 4-HPR encapsulated in O/W emulsions and 4-HPR encapsulated in polymeric micelles were intravenously injected into mice at a dose of 75 mg/kg as 4-HPR on 8, 10, 12 days after tumor inoculation. The dose of empty polymeric micelles was 375 mg/kg as polymer, which was equivalent dose to 4-HPR encapsulation in polymeric micelles. Each value represents the mean \pm S.D. ($n=6-12$). Statistically significant differences compared with PBS-treated groups (** $P < 0.01$; * $P < 0.05$).

three times) after tumor inoculation. Only 4-HPR encapsulated in polymeric micelles significantly delayed tumor growth in B16BL6-bearing mice as compared with PBS (Fig. 5), while did not cause any significant weight loss (data not shown). On 18 days after tumor inoculation, approximately 55% of tumor growth inhibition was observed in mice treated with 4-HPR encapsulated in polymeric micelles. On the other hand, empty polymeric micelles and 4-HPR encapsulated in O/W emulsions did not have any effect on tumor growth (Fig. 5).

Table 1

Pharmacokinetic parameters for blood and tumor concentration of 4-HPR after intravenous injection of 4-HPR encapsulated in polymeric micelles, 4-HPR encapsulated in O/W emulsions, and 4-HPR encapsulated in PEGylated O/W emulsions into B16BL6-bearing mice.

Formulation	$t_{1/2}$ (h)	$AUC_{0-\infty}$ ($\mu\text{g h/mL}$)	Cl_{tot} (mL/h/kg)	V_{dis} (mL/kg)	MRT (h)		
Blood*							
O/W emulsions	1.73	197	382	843	2.21		
PEGylated O/W emulsions	1.73	225	333	737	2.21		
Polymeric micelles	8.68	4717	15.9	199	12.5		
Formulation	C_{max} ($\mu\text{g/g}$)	T_{max} (h)	$t_{1/2}$ (h)	$AUC_{0-\infty}$ ($\mu\text{g h/g}$)	Cl_{tot} (g/h/kg)	V_{dis} (g/kg)	MRT (h)
Tumor							
O/W emulsions	18.7	3	17.7	430	175	4242	14.3
PEGylated O/W emulsions	21.7	1	20.1	509	147	4038	27.4
Polymeric micelles	56.6	6	99.8	7264	10.3	1505	146

$t_{1/2}$ = half-life; AUC = area under the curve; Cl_{tot} = total body clearance; V_{dis} = volume of distribution at steady state; MRT = mean residence time; C_{max} = maximum concentration; T_{max} = time of maximum concentration; parameters were calculated from the mean value of three to six mice by moment analysis developed by Yamaoka et al. (1978).

* Parameters in blood were calculated for the initial phase of the experiment until 6 h after intravenous injection.

4. Discussion

Nano-particulate formulation is very attractive for intravenous injection of lipophilic drugs including 4-HPR. Previously, we have developed poly(ethylene glycol)-poly(aspartate) block copolymer micelles modified with benzyl groups and demonstrated their properties of stable encapsulation and enhanced blood circulation time of 4-HPR in mice (Okuda et al., 2008). In this study, we further investigated its disposition characteristics and pharmacological effects of 4-HPR encapsulated in polymeric micelles in tumor-bearing mice. We demonstrated here for the first time that *in vivo* antitumor effect was achieved by intravenous injection of 4-HPR encapsulated in polymeric micelles.

Spaces in the blood endothelium formed by solid tumors were reported to range between 300 and 4700 nm (Yuan et al., 1995; Hashizume et al., 2000). As shown in Fig. 2, the mean particle size of prepared polymeric micelles was approximately 173 nm. Furthermore, their mean particle size did not change for more than 1 month storage, even at room temperature (data not shown). These results suggested that they might be small enough to exert long circulating potential and pass through the endothelium of solid tumors.

As shown in Fig. 3(A), exposure to 4-HPR for more than 24 h was needed to exert high antitumor activity of 4-HPR against B16BL6 cells *in vitro*. This observation of *in vitro* antitumor characteristics of 4-HPR corresponds with a previous report (Wu et al., 2005) and in the other cancer cells (Holmes et al., 2003). Since EPR effects are known to enhance and prolong tumor distribution based on the characteristic vascular structure around tumor tissues, such passive targeting of 4-HPR to tumor tissues by EPR effects is expected to be an effective strategy for exerting *in vivo* pharmacological actions. After intravenous injection of 4-HPR encapsulated in polymeric micelles, the blood concentration of 4-HPR was extended (Fig. 4(A)). Investigating whether polymeric micelles can improve *in vivo* antitumor efficacy of 4-HPR, and the therapeutic efficacy of 4-HPR encapsulated in polymeric micelles was evaluated in B16BL6-bearing mice. As shown in Fig. 4(B), the tumor concentration of 4-HPR by 4-HPR encapsulated in polymeric micelles was from 33.9 to 56.6 $\mu\text{g/g}$ of 4 HPR for 48 h and could significantly inhibit tumor growth (Fig. 5). The *in vivo* antitumor efficacy might be supported by the fact that *in vitro* IC_{50} value of 4-HPR against B16BL6 cells at more than 24 h was approximately 0.60 $\mu\text{g/mL}$. *In vitro* antitumor activity of 4-HPR encapsulated in polymeric micelles was much lower than that of 4-HPR in free form (Fig. 4(B)), but intravenously injected 4-HPR encapsulated in polymeric micelles showed the enhanced antitumor efficacy *in vivo* (Fig. 5). It might be partly explained that stably encapsulated 4-HPR was much slowly released in medium but was a little enhanced

releasing by interaction with various biocomponents such as serum albumin and blood cells *in vivo*. With regard to the toxicity of 4-HPR encapsulated in polymeric micelles, no significant loss of body weight was observed in treated mice, suggesting little severe toxicity (data not shown). These results lead us to believe that enhanced *in vivo* antitumor efficacy of 4-HPR could be achieved by polymeric micelles without severe side-effects.

Lipid particles are known as conventional drug carriers, and have been already used clinically (Tamilvanan, 2004; Torchilin, 2005). In particular, O/W emulsions or PEGylated O/W emulsions can dissolve highly lipophilic drugs in the inner oil phase; however, few reports are available to compare the disposition of lipophilic drugs by encapsulation into polymeric micelles with that in these emulsions. After intravenous injection of 4-HPR encapsulated in O/W emulsions and PEGylated O/W emulsions, 4-HPR were rapidly eliminated from the blood and tumor (Fig. 4). Similarly, *in vivo* antitumor efficacy by 4-HPR encapsulated in O/W emulsion was not observed (Fig. 5). In our previous study, we systematically investigated the *in vivo* disposition of drugs with diverse lipophilicity, and concluded that the required lipophilicity of drugs for stable encapsulation into O/W emulsions was found to be 10^9 based on the partition coefficient between n-octanol and water (PC_{oct}) values (Takino et al., 1994). PC_{oct} of 4-HPR is $10^{8.03}$ (Kokate et al., 2007); therefore, 4-HPR might be rapidly released from O/W emulsions and PEGylated O/W emulsions to the blood stream by the intravenous injection.

Many factors can contribute to tumorigenesis, including inherited and acquired genetic changes, chromosomal rearrangements, epigenetic phenomena and chemical carcinogenesis. Retinoids can interfere with these events on several levels, their principal known actions being the induction of differentiation and apoptosis of tumor cells, and inhibition of tumor promotion in chemically induced cancers (Means and Gudas, 1995; Kagechika and Shudo, 2005). To date, many retinoids are candidates for the treatment of cancers (Altucci and Gronemeyer, 2001; Clarke et al., 2004); however, it is difficult to achieve therapeutic effect under *in vivo* conditions because their highly lipophilic nature and teratogenicity (Collins and Mao, 1999; Soprano and Soprano, 1995). In order to overcome these problems, we developed poly(ethylene glycol)-poly(benzyl aspartate) block copolymer micelles for 4-HPR delivery. In polymeric micelle delivery, drug encapsulation characteristics can be controlled by modification of the hydrophobic segments of block copolymers (Yokoyama et al., 2004; Watanabe et al., 2006; Okuda et al., 2008). Taking these into consideration, polymeric micelles would be effective carriers for various retinoids for cancer chemotherapy in the future.

In conclusion, we have examined the biodistribution characteristics of 4-HPR encapsulated in poly(ethylene glycol)-poly(benzyl

aspartate) block copolymer micelles after intravenous injection in tumor-bearing mice. We have demonstrated that 4-HPR encapsulated in polymeric micelles sustained blood retention of 4-HPR, passive accumulation at tumor sites, and led to superior therapeutic benefits of 4-HPR against solid tumor in tumor-bearing mice.

Acknowledgements

This work was supported in part by Grants-in-Aid for Scientific Research from the Ministry of Education, Culture, Sports, Science, and Technology of Japan, and by Health and Labour Sciences Research Grants for Research on Advanced Medical Technology from the Ministry of Health, Labour and Welfare of Japan. T. Satoh, Y. Oka, and M. Yokoyama acknowledge support by the Program for Promoting the Establishment of Strategic Research Centers, Special Coordination Funds for Promoting Science and Technology, The Ministry of Education, Culture, Sports, Science, and Technology, Japan.

References

Altucci, L., Gronemeyer, H., 2001. The promise of retinoids to fight against cancer. *Nat. Rev. Cancer* 1, 181–193.

Chansri, N., Kawakami, S., Yamashita, F., Hashida, M., 2006. Inhibition of liver metastasis by all-trans retinoic acid incorporated into O/W emulsions in mice. *Int. J. Pharm.* 321, 42–49.

Chansri, N., Kawakami, S., Yokoyama, M., Yamamoto, T., Charoensit, P., Hashida, M., 2008. Anti-tumor effect of all-trans retinoic acid loaded polymeric micelles in solid tumor bearing mice. *Pharm. Res.* 25, 428–434.

Clarke, N., Germán, P., Altucci, L., Gronemeyer, H., 2004. Retinoids: potential in cancer prevention and therapy. *Expert Rev. Mol. Med.* 6, 1–23.

Collins, M.D., Mao, G.E., 1999. Teratology of retinoids. *Annu. Rev. Pharmacol. Toxicol.* 39, 399–430.

Corazzari, M., Lovat, P.E., Oliverio, S., Di Sano, F., Donnorso, R.P., Redfern, C.P., Piacentini, M., 2005. Fenretinide: a p53-independent way to kill cancer cells. *Biochem. Biophys. Res. Commun.* 331, 810–815.

Hail Jr., N., Kim, H.J., Lotan, R., 2006. Mechanisms of fenretinide-induced apoptosis. *Apoptosis* 11, 1677–1694.

Hashizume, H., Baluk, P., Morikawa, S., McLean, J.W., Thurston, G., Roberge, S., Jain, R.K., McDonald, D.M., 2000. Openings between defective endothelial cells explain tumor vessel leakiness. *Am. J. Pathol.* 156, 1363–1380.

Holmes, W.F., Soprano, D.R., Soprano, K.J., 2003. Comparison of the mechanism of induction of apoptosis in ovarian carcinoma cells by the conformationally restricted synthetic retinoids CD437 and 4-HPR. *J. Cell. Biochem.* 89, 262–278.

Hultin, T.A., May, C.M., Moon, R.C., 1986. N-(4-hydroxyphenyl)-all-trans-retinamide pharmacokinetics in female rats and mice. *Drug Metab. Dispos.* 14, 714–717.

Kagechika, H., Shudo, K., 2005. Synthetic retinoids: recent developments concerning structure and clinical utility. *J. Med. Chem.* 48, 5875–5883.

Kataoka, K., Harada, A., Nagasaki, Y., 2001. Block copolymer micelles for drug delivery: design, characterization and biological significance. *Adv. Drug Deliv. Rev.* 47, 113–131.

Kawakami, S., Opanasopit, P., Yokoyama, M., Chansri, N., Yamamoto, T., Okano, T., Yamashita, F., Hashida, M., 2005. Biodistribution characteristics of all-trans

retinoic acid incorporated in liposomes and polymeric micelles following intravenous administration. *J. Pharm. Sci.* 94, 2606–2615.

Kawakami, S., Suzuki, S., Yamashita, F., Hashida, M., 2006. Induction of apoptosis in A549 human lung cancer cells by all-trans retinoic acid incorporated in DOTAP/cholesterol liposomes. *J. Control. Release* 110, 514–521.

Kokate, A., Li, X., Jasti, B., 2007. Transport of a novel anti-cancer agent, fenretinide across Caco-2 monolayers. *Invest. New Drugs* 25, 197–203.

Kwon, G.S., 2003. Polymeric micelles for delivery of poorly water-soluble compounds. *Crit. Rev. Ther. Drug Carrier Syst.* 20, 357–403.

Maeda, H., 2001. The enhanced permeability and retention (EPR) effect in tumor vasculature: the key role of tumor-selective macromolecular drug targeting. *Adv. Enzyme Regul.* 41, 189–207.

Means, A.L., Gudas, L.J., 1995. The roles of retinoids in vertebrate development. *Annu. Rev. Biochem.* 64, 201–233.

Miller Jr., W.H., 1998. The emerging role of retinoids and retinoic acid metabolism blocking agents in the treatment of cancer. *Cancer* 83, 1471–1482.

Moon, R.C., Thompson, H.J., Becci, P.J., Grubbs, C.J., Gander, R.J., Newton, D.L., Smith, J.M., Phillips, S.L., Henderson, W.R., Mullen, L.T., Brown, C.C., Sporn, M.B., 1979. N-(4-hydroxyphenyl)retinamide, a new retinoid for prevention of breast cancer in the rat. *Cancer Res.* 39, 1339–1346.

Okuda, T., Kawakami, S., Yokoyama, M., Yamamoto, T., Yamashita, F., Hashida, M., 2008. Block copolymer design for stable encapsulation of N-(4-hydroxyphenyl)retinamide into polymeric micelles in mice. *Int. J. Pharm.* 357, 318–322.

Opanasopit, P., Yokoyama, M., Watanabe, M., Kawano, K., Maitani, Y., Okano, T., 2004. Block copolymer design for camptothecin incorporation into polymeric micelles for passive tumor targeting. *Pharm. Res.* 21, 2001–2008.

Soprano, D.R., Soprano, K.J., 1995. Retinoids as teratogens. *Annu. Rev. Nutr.* 15, 111–132.

Swanson, B.N., Zaharevitz, D.W., Sporn, M.B., 1980. Pharmacokinetics of N-(4-hydroxyphenyl)-all-trans-retinamide in rats. *Drug Metab. Dispos.* 8, 168–172.

Takino, T., Konishi, K., Takakura, Y., Hashida, M., 1994. Long circulating emulsion carrier systems for highly lipophilic drugs. *Biol. Pharm. Bull.* 17, 121–125.

Tamilvanan, S., 2004. Oil-in-water lipid emulsions: implications for parenteral and ocular delivering systems. *Prog. Lipid Res.* 43, 489–533.

Torchilin, V.P., 2004. Targeted polymeric micelles for delivery of poorly soluble drugs. *Cell. Mol. Life Sci.* 61, 2549–2559.

Torchilin, V.P., 2005. Recent advances with liposomes as pharmaceutical carriers. *Nat. Rev. Drug Discov.* 4, 145–160.

Villablanca, J.G., Krailo, M.D., Ames, M.M., Reid, J.M., Reaman, G.H., Reynolds, C.P., 2006. Phase I trial of oral fenretinide in children with high-risk solid tumors: a report from the Children's Oncology Group (CCG 09709). *J. Clin. Oncol.* 24, 3423–3430.

Watanabe, M., Kawano, K., Yokoyama, M., Opanasopit, P., Okano, T., Maitani, Y., 2006. Preparation of camptothecin-loaded polymeric micelles and evaluation of their incorporation and circulation stability. *Int. J. Pharm.* 308, 183–189.

Wu, X.Z., Zhang, L., Shi, B.Z., Hu, P., 2005. Inhibitory effects of N-(4-hydroxyphenyl)retinamide on liver cancer and malignant melanoma cells. *World J. Gastroenterol.* 11, 5763–5769.

Yamaoka, K., Nakagawa, T., Uno, T., 1978. Statistical moments in pharmacokinetics. *J. Pharmacokinet. Biopharm.* 6, 547–558.

Yamaoka, K., Tanigawara, Y., Nakagawa, T., Uno, T., 1981. A pharmacokinetic analysis program (multi) for microcomputer. *J. Pharmacobiodyn.* 4, 879–885.

Yokoyama, M., Opanasopit, P., Okano, T., Kawano, K., Maitani, Y., 2004. Polymer design and incorporation methods for polymeric micelle carrier system containing water-insoluble anti-cancer agent camptothecin. *J. Drug Target* 12, 373–384.

Yuan, F., Dellian, M., Fukumura, D., Leunig, M., Berk, D.A., Torchilin, V.P., Jain, R.K., 1995. Vascular permeability in a human tumor xenograft: molecular size dependence and cutoff size. *Cancer Res.* 55, 3752–3756.



Encapsulation of the synthetic retinoids Am80 and LE540 into polymeric micelles and the retinoids' release control

Taku Satoh^a, Yuriko Higuchi^b, Shigeru Kawakami^b, Mitsuru Hashida^b, Hiroyuki Kagechika^c, Koichi Shudo^d, Masayuki Yokoyama^{a,*}

^a Yokoyama Project, Kanagawa Academy of Science and Technology, KSP East 404, Sakado 3-2-1, Takatsu-ku, Kawasaki, Kanagawa 213-0012, Japan

^b Department of Drug Delivery Research, Graduate School of Pharmaceutical Sciences, Kyoto University, Sakyo-ku, Kyoto 606-8501, Japan

^c School of Biomedical Science, Tokyo Medical and Dental University, Kanda-jurugodai 2-3-10, Chiyoda-ku, Tokyo 101-0062, Japan

^d Research Foundation Itsuu Laboratory, Tamagawa 2-28-10, Setagaya-ku, Tokyo 158-0094, Japan

ARTICLE INFO

Article history:

Received 25 December 2008

Accepted 27 February 2009

Available online xxx

Keywords:

Polymeric micelle

Retinoid

Ion-pairing

Sustained release

Controlled release

ABSTRACT

The objective of this study was to encapsulate two synthetic retinoids Am80 and LE540 into polymeric micelles and to control the retinoids' release rate in vitro. Highly efficient encapsulation yields of these retinoids were obtained for micelles forming from PEG-poly(benzyl aspartate) block copolymers in the wide range of the benzyl substitution degree. The in vitro release examination for LE540 indicated very stable encapsulation of this retinoid owing to its strongly hydrophobic nature. On the other hand, Am80 exhibited a rapid release in Dulbecco's phosphate buffer saline. An addition of a hydrophobic alkyl amine in the Am80-encapsulation process successfully led to significant retardation of the Am80 release rate. A mechanism of the retardation was considered an increase of Am80 hydrophobicity due to an ion-pairing with the alkyl amine. This paper is the first report on release control in the polymeric micelle carrier system through the ion-pairing between an encapsulated drug and an additive.

© 2009 Published by Elsevier B.V.

1. Introduction

Polymeric micelles are self-assembling nanostructures that are typically composed of amphiphilic block copolymers [1]. Micelles have recently received much attention as a promising drug delivery carrier because a large quantity of hydrophobic drugs can be encapsulated into the micelle core in a stable manner. In systemic administration the drug-encapsulating micelles are expected to demonstrate various advantages; e.g., long circulation in the blood stream owing to the nano-size and the hydrated-surface property of the micelles, and selective accumulation at tumor tissues owing to the EPR effect [2].

For drug targeting with the polymeric micelle carriers, research and development have focused on hydrophobic and cytotoxic anti-cancer drugs such as doxorubicin [3], paclitaxel [4], and camptothecin and its analogues [5,6]. These drugs cause cell mortality by means of strong cellular dysfunction. We would like to explore an application of polymeric micelle delivery using another type of drug that expresses pharmacological activities by regulating cellular functions. We have selected retinoids for this purpose [7,8].

Retinoids were originally defined as vitamin A and its analogues [9]. Compounds in this family modulate specific nuclear receptors

called retinoic acid and retinoid X receptors (RARs and RXRs). Each of these receptors includes three subtypes (α , β , and γ). By binding to these receptors retinoids regulate cellular events including differentiation, proliferation, and apoptosis [10,11]. All-trans retinoic acid (ATRA) is clinically approved against acute promyelocytic leukemia (APL). This is the first approval of the differentiation therapy against cancer, indicating retinoids' high potency in clinical applications [12]. In an updated definition, retinoids are expanded to include molecules that bind to RARs and RXRs [13,14], regardless of their similarity in molecular structure to vitamin A. Researchers have reported that synthetic retinoids, such as 6-[3-(1-adamantyl)-4-hydroxyphenyl]-2-naphthalene carboxylic acid (CD437) [15] and *N*-(4-hydroxyphenyl) retinamide (4-HPR) [16], have induced apoptosis in neoplasia. Although researchers have not yet fully elucidated the mechanism underlying the related actions of these synthetic retinoids, CD437- and 4-HPR-induced apoptosis includes a RAR-independent pathway. Many other synthetic retinoids have been designed to improve pharmacological effects and to decrease adverse effects [17,18].

For the current research project, we selected two synthetic retinoids, Am80 and LE540, as encapsulated drugs (Chart 1). One reason for our decision to select these retinoids is their attractive pharmacological activities. Am80, an RAR- α/β specific agonist, was approved in Japan in 2005 for relapsed or refractory APL [19]. Its antimyeloma [20] and atherosclerosis inhibition effects in vivo have also been reported [21]. Since this synthetic retinoid has little binding affinity to cellular retinoic acid-binding proteins (CRABP),

* Corresponding author.

E-mail address: yp.yokoyama2093ryo@newkast.or.jp (M. Yokoyama).

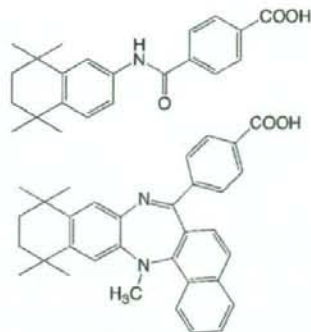


Chart 1. Am80 and LE540 (top and bottom).

CRABP-dependent retinoid-resistance will be avoided. Moreover, Am80 is much more stable than ATRA in the contexts of light, heat, and oxidation. In comparison, LE540 is an RAR antagonist, and its inhibition activity for Am80-induced HL-60 cell differentiation has been reported [22]. Targeting and the controlled release of these retinoids through micelle encapsulation will expand their therapeutic applications, especially when the target is solid tumor tissue for Am80.

Chemical-structure characteristics of Am80 and LE540 constitute the other reason for the selection. We use the hydrophobic frames of these retinoids to encapsulate the compounds into micelles. As compared with Am80, LE540 has bulkier hydrophobic moiety. Therefore, these two retinoids not only possess high therapeutic potential, but also benefit analysis on relations between the chemical structures of drugs and the corresponding encapsulation-release behaviors of the retinoids.

In this study, we perform encapsulation of Am80 and LE540 into micelles forming from PEG-poly(benzyl aspartate) block copolymers and analyze the retinoids' encapsulation behaviors and release rates. Am80 and LE540 are sufficiently hydrophobic in water for easy and efficient encapsulation into a polymeric micelle. However, Am80 is soluble in Dulbecco's phosphate buffered saline (D-PBS) and is rapidly released from a polymeric micelle. Therefore we have attempted to control the release rates by means of an addition of hydrophobic compounds interacting with Am80. This is a novel methodology for the control of drug-release rates from polymeric micelle carriers. Even though addition of oppositely charged hydrophobic compounds have been frequently used in traditional drug carriers such as microparticles, the first time application of this method for the polymeric micelle carriers is very important. The reason for the importance is that extremely stable drug encapsulation (e.g., 10^{-19} cm²/s diffusion coefficient [23]) is required due to a very small micellar inner core such as 10 nm in diameter as a drug container.

2. Materials and methods

2.1. Materials and equipment

For the present study, α -methoxy- ω -amino poly(ethylene glycol) (MeO-PEG-NH₂) (Mw 5-kDa) was purchased from NOF Corp. (Tokyo, Japan). And β -benzyl β -aspartate was purchased from Kokusan Chemical (Tokyo, Japan). Triphosgene was obtained from Tokyo Chemical Industry Co., Ltd. (Tokyo, Japan) and used as received. β -Benzyl β -aspartate *N*-carboxyanhydride (BLA-NCA) was prepared from β -benzyl β -aspartate and triphosgene according to the conventional method [24]. DMF was distilled at a reduced pressure before use. All other reagents used were of reagent grade. ¹H-NMR measurements were carried out with a Varian Unity Inova NMR spectrometer (Varian Technologies Japan Ltd., Tokyo, Japan) at 400 MHz. A Spectra/Por 6 dialysis membrane (Spectrum Laboratories Inc., CA, USA) (1-kDa cut-off) was used for dialysis. An HPLC analysis was carried out with an HPLC system (PU-2080 plus pump; MX-2080-32 dynamic mixer; UV-2070 plus UV detector; and RI-2031 plus RI detector, Jasco Corp., Tokyo, Japan) equipped with a TSK-gel ODS-80Ts reverse-phased column (150 × 4.6 mm i.d., Tosoh Corp., Tokyo, Japan). Dynamic light scattering (DLS) measurements were performed in 1.0% (w/w) aqueous solutions at 25 °C with a DLS-7000 (Otsuka Electronic Co. Ltd., Osaka, Japan). Particle size distribution in terms of weight fractions was calculated using a non-negative least squares (NNLS) algorithm.

2.2. Synthesis of amphiphilic diblock copolymers

Polymers used for encapsulation of retinoids are composed of a PEG-poly(aspartic acid) (PEG-P(Asp)) main chain and pendant benzyl groups (Table 1). PEG-poly(benzyl β -aspartate) (PEG-PBLA) polymers **1** and **2** were prepared by ring-opening polymerization of BLA-NCA from a primary amino terminal of MeO-PEG-NH₂ [25]. The PEG-P(Asp (Bzl))_n polymers **3–5** were obtained as follows: (1) complete removal of benzyl groups from PEG-PBLA [26], and (2) partial esterification of PEG-P(Asp) with benzyl bromide (BzBr) [27].

2.2.1. Synthesis of PEG-*b*-poly(β -benzyl β -aspartate) (PEG-PBLA)

PEG-*b*-poly(β -benzyl β -aspartate) (PEG-PBLA) block copolymers were synthesized according to literature [25]. Amino-terminated poly(ethylene glycol) MeO-PEG-NH₂ as a macroinitiator was mixed with BLA-NCA in a dichloromethane-DMF mixed solvent (9:1 v/v), and this mixture was stirred at 35 °C for 17 h under a nitrogen atmosphere. The reaction mixture was dropwisely added into diethyl ether cooled in ice. The resulting precipitate was collected by filtration, washed with diethyl ether, and dried under a reduced pressure. The degree of polymerization (DP, i.e., the average unit number of polymer chain) of the PBLA block was determined by ¹H-NMR spectroscopy in chloroform-*d*. The determination was based on an integration ratio between the proton assigned to the methylene of PEG (3.8–3.4 ppm) and the benzyl methylene of PBLA (5.2–4.9 ppm). The polymers **1** and **2** were estimated to be **24** and **28**, respectively.

Table 1
Synthesis of PEG-P(Asp (Bzl))_n block copolymers.

Polymer	Source			Product			
	PEG-P(Asp) ^a g (Asp mmol)	BzBr g (mmol)	mol.eq./Asp	DBU g (mmol)	BnBr/ DBU	Yield (mg)	D.s. BzI ^b (%)
3	0.501 (1.51)	0.261 (1.52)	1.01	0.200 (1.31)	0.87	0.597	80
4	0.501 (1.51)	0.172 (1.00)	0.66	0.141 (0.93)	0.61	0.531	53
5	0.501 (1.51)	0.115 (0.67)	0.44	0.093 (0.61)	0.40	0.516	33

^a PEG-P(Asp) 5-24 was prepared by hydrolysis of PEG-PBLA 2.

^b Degree of benzyl substitution.

Please cite this article as: T. Satoh, et al., Encapsulation of the synthetic retinoids Am80 and LE540 into polymeric micelles and the retinoids' release control, J. Control. Release (2009), doi:10.1016/j.jconrel.2009.02.024

2.2.2. Synthesis of PEG-*b*-poly(aspartic acid) (PEG-*P*(Asp))

Benzyl ester of PEG-PBLA **2** was hydrolyzed in 0.5 M aqueous sodium hydroxide solution (3 mol.eq. to benzyl group) at r.t. In approximately 20 min, a suspension of the polymer changed into a transparent solution owing to hydrolysis. The resulting solution was acidified with 6 M hydrochloric acid, dialyzed against water, and freeze-dried. Chemical structures of products were analyzed by ¹H-NMR spectroscopy in deuterium oxide containing sodium deuterioxide. The peaks assigned to the benzyl group completely disappeared on the spectrum, indicating hydrolysis of the benzyl ester. The DP of the poly(aspartic acid) chain decreased from 28 to 24 in this step. It was also confirmed that the α-amide bond in the PBLA main chain was converted into the mixture of α- and β-amides (ca. 1:3) as described in previous reports [26,28].

2.2.3. Synthesis of partially benzyl-substituted PEG-*P*(Asp) (PEG-*P*(Asp)(Bzl)_x)

Partially benzyl-substituted PEG-*P*(Asp) (PEG-*P*(Asp)(Bzl)_x) polymers **3–5** were obtained by esterification of PEG-*P*(Asp) with benzyl bromide in the presence of 1,8-diazabicyclo[5.4.0]undec-7-ene (DBU) as reported in a previous paper [29]. The number *x* in the PEG-*P*(Asp)(Bzl)_x formula represents a percentage (%) of benzyl ester in the aspartic acid residues. PEG-*P*(Asp) was dissolved to DMF and was added by means of BzlBr and DBU, and the reaction mixture was stirred at 50 °C for 16 h under a nitrogen atmosphere. Polymers **3**, **4**, and **5** were obtained when BzlBr was added in 1.01, 0.66, and 0.44 mol. eq. to the aspartic acid unit, respectively, while the BzlBr/DBU mole ratio was almost constant ca. 1.1. The reaction mixture was dropwisely added into diethyl ether. The resulting precipitate was collected by filtration, washed with diethyl ether, and dried under a reduced pressure. For removal of DBU, the polymers were dissolved into DMF, followed by the addition of 6 M hydrochloric acid (1 mol.eq. to DBU), and then this mixture solution was dialyzed against water. The purified products were freeze-dried and analyzed by ¹H-NMR spectroscopy in DMSO-*d*₆ containing 3% trifluoroacetic acid. Table 1 summarizes the degree of benzyl substitution determined from a proton integration ratio between methylene of PEG (3.7–3.4 ppm) and methylene of the benzyl group (5.1–5.0 ppm).

2.3. Preparation of micelles

Drug-encapsulating micelles were obtained by a solvent evaporation method [30]. The process was as follows: the block copolymer (20 mg) and the drug (2.0 mg) were dissolved in THF (2.5 mL). Evaporation of THF with stirring at 40 °C under a dry nitrogen-gas flow provided a residue of the polymer and the drug as a thin-film. The residue was further dried under a reduced pressure, and then added by water (4.0 mL). A drug-encapsulating micelle was formed by subsequent sonication with a VCX-750 sonicator equipped with a 5 mm diameter microtip (Sonic & Materials Inc., CT, USA). The sonication was operated at 21% amplitude with 80-cycle of a 0.5 s pulse followed by a 1.0 s pause, at r.t. The micelle solution was centrifuged to remove a possible insoluble precipitate (3900 rpm, 10 min, 20 °C) and then filtered through a Milllex 0.22 μm PVDF filter (Nihon Millipore K.K., Tokyo, Japan). The obtained micelle solution was stored at –30 °C before use. Empty micelles were prepared according to the same procedure in the absence of drug. When an additive compound was used, the compound was mixed in the initial polymer-drug solution.

2.4. Measurements of drugs encapsulated in micelles

Drug amounts recovered in the micelle solutions were determined by reversed phase HPLC. The mobile phase involved methanol–5% acetic acid aqueous solution mixture at 2:1 (v/v) for Am80 and 9:1 (v/v) for LE540. A flow rate was 1.0 mL/min at 40 °C. Detection was

carried out by absorption at 290 nm and 356 nm for Am80 and LE540, respectively.

2.5. *In vitro* drug release

The drug-encapsulating micelle solution (1.0 mL) was filled in a dialysis tube and dialyzed against 100-fold volume of water or Dulbecco's phosphate buffer saline (D-PBS, pH 7.4) with stirring at r.t. An aliquot of the dialysate was freeze-dried prior to the addition of methanol (100 μL). After centrifugation (10,000 g, 10 min, r.t.), the resulting supernatant was applied to the reverse-phase HPLC system for measurements of the released drugs. This drug-release assay was performed in triplicate except as described elsewhere. The error bars represent the standard deviation.

2.6. Measurements of *N,N*-dimethyldodecylamine (DMDA) encapsulated in micelles

The micelles of polymer **1** (20 mg) were prepared through the evaporation-sonication process in the presence of Am80 (2.0 mg, 5.69 μmol) and *N,N*-dimethyldodecylamine (DMDA, 1.2 mg, 5.69 μmol) in water (4.0 mL). After the centrifugation and filtration, the resulting solution (500 μL) was ultrafiltered (10,000 g, 25 min, r.t.) with a Microcon YM-100 centrifugal filter unit (Nihon Millipore K.K., Tokyo, Japan). Fresh water (200 μL) was added to a retentate and ultrafiltered again (10,000 g, 20 min, r.t.). This water-addition-ultrafiltration cycle was repeated three times. The retentate and the filtrate were collected and their contents of Am80 and DMDA were determined by means of a reversed-phase HPLC. Measurement conditions for DMDA were as follows: the mobile phase was methanol–water at 9:1 (v/v) containing 0.1% (v/v) of triethylamine, the flow rate was 1.0 mL/min at 40 °C, and detection of DMDA was carried out with an RI detector. This experiment was performed in triplicate. The other sample solutions containing different compositions were prepared for the comparison as shown in Table 5.

2.7. Statistics

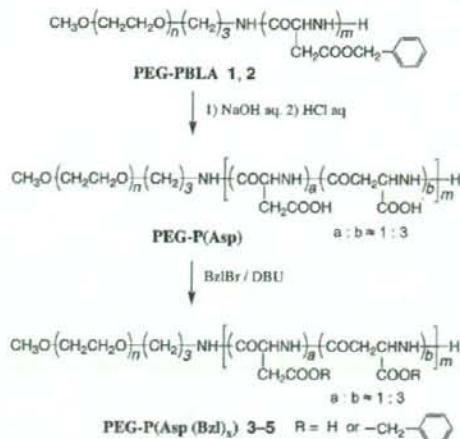
Each release study was performed in triplicate except for specifically indicated cases. Data were expressed as the mean ± standard deviation (SD). Statistical comparisons were performed by the use of two-tailed Student's *t*-test for two-groups, and Dunnett's method by the use of a JMP Version 6 Japanese edition software (SAS Institute Japan, Tokyo) for multiple groups.

3. Results and discussion

3.1. Preparation of drug-encapsulating micelles

PEG-PBLA polymers **1** and **2** were successfully prepared according to literatures (see experimental section). Polymer **2** was converted into PEG-*P*(Asp)(Bzl)_x **3–5** through hydrolysis of **2** and subsequent benzyl-esterification (Scheme 1). The degree of benzyl substitution of **3–5** was controlled with feed amounts of BzlBr and DBU (Table 1). The micelles from polymers **1** and **3–5** were obtained by means of the solvent evaporation-sonication technique. The evaporation process resulted in formation of a thin film composed of a mixture of polymer and drug. Subsequent sonication of this film in water provided a drug-encapsulating polymeric micelle solution.

It is worth pointing out that both Am80 and LE540 were very efficiently encapsulated in the PEG-PBLA and PEG-*P*(Asp)(Bzl)_x polymer micelles (Table 2). A high encapsulation yield of ≥75% of the feed was demonstrated on all polymers examined in the wide range of 33 to 100% of the degree of benzyl substitution. Any precipitate was not formed, and furthermore, insoluble aggregates did not interfere with the filtration. When PEG-*P*(Asp)(Bzl)_x polymers



Polymer	n	m	D.s. Bzl* (%)
1	117	24	100
2	117	28	100
3	117	24	80
4	117	24	53
5	117	24	33

* Degree of benzyl substitution.

Scheme 1. Synthetic scheme of PEG-P(Asp (Bzl)_a) from PEG-PBLA.

encapsulated a hydrophobic drug, camptothecin, the benzyl substitution degree significantly affected the drug encapsulation efficiency [29]. It was reported that an encapsulation yield of camptothecin reached >90% at 69% of the benzyl substitution degree, however, the yield decreased to <40% at 44% of the substitution. In contrast, Am80 and LE540 were encapsulated at high yields in a wide range of the benzyl ester content of PEG-P(Asp (Bzl)_a).

Transparent solutions from polymers 3 and 4 and very faintly hazy ones from polymers 1 and 5 were obtained by means of the evaporation-sonication technique in the presence of a drug. It is important to note that Am80 and LE540 themselves were almost insoluble in water. When the evaporation-sonication technique was applied to the drugs without a polymer, only a slight amount of the drugs (<1% of the feed) was detected in supernatants after the centrifugation. The remaining part of the feed drugs was separated as precipitates. These results indicated that the faintly hazy appearance of the micelle solutions from polymers 1 and 5 was due to particle

sizes \geq ca. 140 nm of the polymeric micelles (Table 2), not due to dispersed free drug aggregates.

Interestingly, very low intensity of scattered light was observed in a DLS measurement for a solution of polymer 5 through the evaporation-sonication process without a drug. This result indicated that polymer 5 alone did not form micelle structures as clearly as polymers 1, 3, and 4 owing to its low degree (33%) of hydrophobic benzyl substitution. This block copolymer 5 obtained sufficient hydrophobicity to distinctly form micellar structures by physically entrapping the hydrophobic drug. This preferential contribution of the encapsulated drug to the micelle formation can expand choices of block copolymer compositions. Block copolymers possessing hydrophobicity insufficient for the micelle formation can be used for micelle drug-carrier systems if these polymers are successfully given additional hydrophobicity by the encapsulated drugs. This was reported for chemical conjugation of drugs to block copolymers [31], in a doxorubicin-conjugated PEG-P(Asp) system. In contrast, for this Am80 case, the drug was encapsulated in a much easier way, physical entrapment. As far as we know, this is the first report regarding this type of preferential contribution of the physically entrapped drug to polymeric micelles' formation.

3.2. Drug release from micelles in vitro

In vitro drug-release rates were measured by means of a dialysis method. The sealed dialysis bag containing the drug-encapsulating micelle solution was placed in a container of D-PBS or water. Using HPLC, we monitored the drug's release from the micelles into an aqueous medium outside the dialysis bag. The experiments were carried out by the use of the micelle solutions summarized in Table 2. These micelle solutions contained Am80 and LE540 in the concentration range of 0.37–0.53 mg/mL and 0.41–0.54 mg/mL, respectively.

A rapid release of Am80 occurred in D-PBS. Approximately 60% of the encapsulated Am80 was released within 8 h for all polymers as shown in Fig. 1. We observed no influence of the polymers' benzyl substitution degree on the release rate. Am80 was soluble in D-PBS at $\geq 200 \mu\text{g/mL}$ at r.t. as opposed to Am80's poor solubility of $2 \mu\text{g/mL}$ in water under the same conditions. Such high solubility in D-PBS is likely to accelerate the rapid release. The observed release rates in this evaluation seem to be too fast for drug targeting purposes, since a blood-circulation period of 24 h or more was necessary for the EPR effect's efficient passive targeting to a solid tumor tissue [2]. The rapid drug-release behaviors shown in Fig. 1 suggest a situation where most of the encapsulated drug is released in the blood stream before the drug carrier system accumulates at the tumor tissue.

Table 2
Encapsulation yield of the drugs and particle size distributions of the polymeric micelles.^a

Polymer	Am80 encapsulation		LE540 encapsulation		Empty
	% Drug encapsulated	Particle size (nm); weight fraction	% Drug encapsulated	Particle size (nm); weight fraction	Particle size (nm); weight fraction
1	94	42 ± 9; 81%	82	52 ± 10; 71%	60 ± 28; 100%
2		151 ± 29; 19%		148 ± 28; 29%	
3	105	21 ± 4; 100%	109	17 ± 3; 92%	7 ± 1; 85%
4	101	20 ± 4; 100%	100	73 ± 13; 8%	21 ± 4; 15%
5	75	188 ± 37; 94%	94	23 ± 5; 100%	17 ± 3; 100%
		817 ± 91; 6%		54 ± 8; 66%	– ^b
				137 ± 24; 34%	

^a Weight distributions.

^b Very low intensity of scattered light.

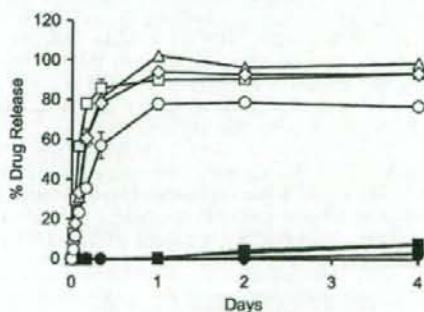


Fig. 1. Release of Am80 and LE540 from the polymeric micelles at r.t. in D-PBS (mean \pm SD, $n = 3$). The drug-encapsulating micelles were prepared from polymer 1 (circle), 3 (diamond), 4 (triangle), and 5 (square). Open and filled symbols indicate Am80 and LE540, respectively. The amounts of drug encapsulated in polymeric micelles were normalized to 100%.

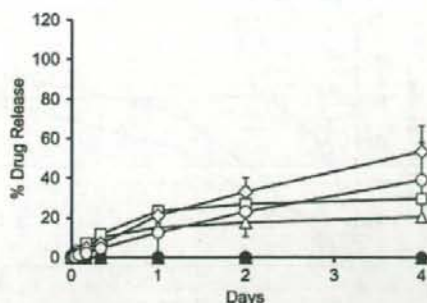


Fig. 2. Release of Am80 and LE540 from the polymer micelles at r.t. in water (mean \pm SD, $n=3$). The drug-encapsulating micelles were prepared from polymer 1 (circle), 3 (diamond), 4 (triangle), and 5 (square). Open and filled symbols indicate Am80 and LE540, respectively. The amounts of drug encapsulated in polymeric micelles were normalized to 100%.

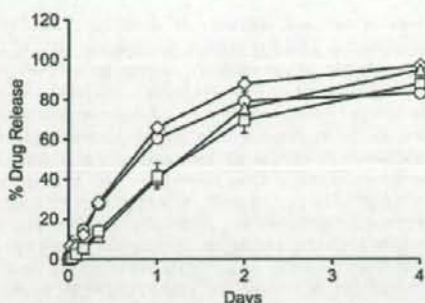


Fig. 3. Release of Am80 from the polymeric micelles at r.t. in D-PBS (mean \pm SD, $n=3$). The Am80-encapsulating micelles were prepared from polymer 1 (circle), 3 (diamond), 4 (triangle), and 5 (square) in the presence of DMDA at various molar ratios to Am80 (circle=1, diamond=2.7, triangle=5.4, and square=7.5). The amounts of drug encapsulated in polymeric micelles were normalized to 100%.

As compared with the release in D-PBS, considerable release retardation of Am80 was observed in water as shown in Fig. 2. Accumulated Am80 release amounts after 8 h were only 5–12%. Even 4 days later, the released Am80 amounts remained in a range of 20–53%. These results demonstrated that the release rates of Am80 in D-PBS as a dialysate were dramatically differed from the release rates to Am80 in water as a dialysate. This difference was probably due to a difference in Am80 solubility in these solvents. In the release experiments in water, small amounts of powdery precipitates appeared in the dialysis bag within 1–2 days except for the micelles of polymer 1. This precipitate seems to have been the released Am80. The poor solubility of Am80 in water is likely to lead to saturation in the dialysis bag prior to Am80's diffusion into the exterior. All these results imply that the poor Am80 solubility in water favors very high encapsulation efficiency, and that the higher solubility in D-PBS than in water causes a rapid release of Am80 from micelles.

In contrast, LE540 was scarcely released either in D-PBS or in water throughout the time period examined, indicating LE540's very stable encapsulation of the synthetic retinoid into the polymeric micelles, as shown in Figs. 1 and 2. Only 3–8% of release was observed in D-PBS over the course of 4 days. This stable encapsulation probably resulted from stronger hydrophobicity of LE540 than of Am80.

3.3. Addition of *N,N*-dimethyldodecylamine (DMDA)

To accomplish more stable encapsulation of Am80, we investigated complex formation of Am80 with a hydrophobic additive. A hydrophobic fatty amine was selected for this purpose. First, *N,N*-dimethyldodecylamine (DMDA) was mixed with Am80 and the polymer in THF, and the mixture was applied to the evaporation-

sonication process for the encapsulation. The molar ratio of DMDA to Am80 (DMDA/Am80) was adjusted to 1.0, 2.7, 5.4, and 7.5 for the micelles of polymers 1, 3, 4, and 5, respectively. These amounts of DMDA corresponded to the molar equivalent of all carboxyl groups of Am80 and aspartic acid residue of a polymer. High Am80 encapsulation yields >94% were confirmed (Table 3; Entries 1, 5, 7, and 9), indicating that the presence of DMDA did not lower the drug encapsulation efficiency. The particle sizes of the polymeric micelles prepared with DMDA did not show a substantial change compared with those prepared without this additive (Table 3; Entries 1, 5, and 7). The only exception was the case of polymer 5, where the particle diameter decreased from ca. 200 nm to <10 nm upon the addition of DMDA (Table 3; Entry 9). This unique result was found only for polymer 5, which exhibited distinctive micelle formation only after encapsulation of Am80. (As described above, only polymer 5 did not form a micelle structure.) Although the mechanism for this behavior has not been elucidated, this exceptional result was not observed for the other polymers that formed micelle structures even in the absence of the encapsulated drug.

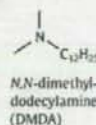
A remarkable effect of the DMDA addition was a significant retardation in Am80 release from the polymeric micelles in D-PBS, as shown in Fig. 3. A period of 2 days was necessary to attain 60% release of the encapsulated Am80, while the same amounts were rapidly released within 8 h in the absence of DMDA (Fig. 1). At 8 h of the release period, the retardation of Am80 release by means of the DMDA addition indicated statistically significant differences ($P<0.05$) in each polymeric micelle as compared with each micelle without the DMDA addition.

Two mechanisms should be considered to explain these results. The first is a hydrophobic complex formation of Am80 between DMDA. A hydrophilic carboxylic group of Am80 is assumed to greatly

Table 3
Encapsulation of Am80 into the polymeric micelles in the presence of DMDA.

Entry	Polymer	DMDA/Am80 ^a	% Am80 encapsulated	Particle size (nm); weight fraction
1	1	1	94	36 \pm 4; 56%; 135 \pm 26; 24%; 639 \pm 110; 20%
2	1	2.7	97	43 \pm 8; 77%; 135 \pm 25; 17%
3	1	5.4	103	66 \pm 24; 89%; 679 \pm 109; 11%
4	1	7.5	101	54 \pm 14; 77%; 817 \pm 102; 23%
5	3	2.7	97	14 \pm 0; 64%; 32 \pm 7; 35%; 817 \pm 102; 1%
6	4	1	100	24 \pm 7; 100%
7	4	5.4	101	13 \pm 2; 97%; 39 \pm 8; 3%
8	4	10.7	90	22 \pm 4; 100%
9	9	7.5	104	4 \pm 0; 74%; 8 \pm 1; 26%

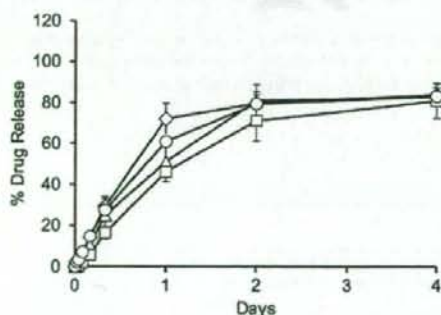
^a Molar ratio.



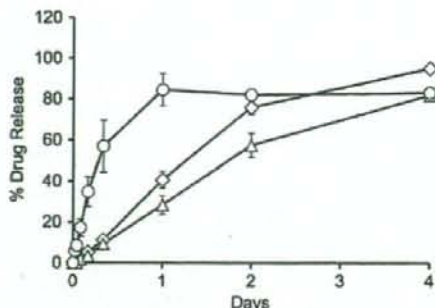
403 contribute to the high solubility of Am80 in D-PBS. Therefore,
 404 conversion of this group to a more hydrophobic state is probably
 405 effective in decreasing the solubility. An ionic compound's solubility
 406 can be changed by means of an electrostatic interaction between an
 407 opposite charged hydrophobic compound, and researchers have used
 408 the effect as the "hydrophobic ion-pairing" technique [32,33]. This
 409 technique serves to increase the hydrophobicity of hydrophilic ionic
 410 compounds including a drug [33,34] as well as a protein and
 411 polynucleotide [32]. For example, a potent antituberculosis drug,
 412 isonicotinic acid hydrazide, was chemically converted into an ionic
 413 compound as a prodrug, and the hydrophobic ion-pairing significantly
 414 enhanced drug's solubility to an organic solvent [33]. Furthermore,
 415 skin accumulation of retinoic acid was enhanced by an ion-pairing
 416 with a series of hydrophobic amino acid methyl esters [34]. In our
 417 study, DMDA is regarded as a hydrophobic counter partner for Am80.
 418 This is the first report that the ion-pairing technique has been used for
 419 stable drug encapsulation in the polymeric micelle carrier system.

420 The second mechanism that explains the effect of DMDA is a change
 421 of micellar core characteristics by encapsulation of a hydrophobic
 422 additive. Forrest et al. reported that encapsulation of α -tocopherol
 423 (vitamin E) into PEG-*b*-poly(ϵ -caprolactone) (PEG-PCL) micelles
 424 decreased the viscosity of the crystalline PCL core owing to dispersed
 425 microphases of α -tocopherol [23]. Such a plasticized PCL core was
 426 receptive to a larger amount of rapamycin loading. Furthermore, the α -
 427 tocopherol-co-encapsulating micelle demonstrated a retardation of
 428 the drug release in PBS containing bovine serum albumin as compared
 429 with the PEG-PCL micelle formed without α -tocopherol.

430 If DMDA contributes to the sustained release of Am80 mainly by
 431 means of the hydrophobic ion-pairing, this contribution increases
 432 up to the DMDA addition at the DMDA/Am80 molar ratio of 1. On the
 433 other hand, if DMDA acts to change the characteristics of the micellar
 434 core, the retardation effect by DMDA relies on the amount of added
 435 DMDA beyond the DMDA/Am80 ratio of 1. Therefore, we investigated
 436 the effects of an added DMDA amount by using polymers 1 and 4.
 437 When DMDA was added to a mixture of polymer 1 and Am80 in the
 438 range of the DMDA/Am80 ratio from 1.0 to 7.5 (Table 3; Entries 1–4),
 439 the drug-release rate underwent no significant changes, as shown in
 440 Fig. 4. This result indicated that the retardation of the Am80 release
 441 was due to the hydrophobic ion-pairing of Am80 and DMDA for the
 442 polymer 1 case. On the other hand, the retardation of the drug release
 443 was observed at the DMDA/Am80 ratio ≥ 5.4 for the micelle of polymer
 444 4 as shown in Fig. 5. The retardation effect hardly exhibited itself at the



445 Fig. 4. Release of Am80 from the micelles of polymer 1 at r.t. in D-PBS (mean \pm SD,
 446 $n = 3$). The Am80-encapsulating micelles were prepared in the presence of DMDA
 447 at various molar ratios to Am80 (circle = 1, diamond = 2.7, triangle = 5.4, and
 448 square = 7.5). The result at the ratio of 1 represented in Fig. 3 was shown again for
 449 the comparison with the results at the other ratios. The amounts of drug encapsulated
 450 in polymeric micelles were normalized to 100%.



445 Fig. 5. Release of Am80 from the micelles of polymer 4 at r.t. in D-PBS (mean \pm SD,
 446 $n = 3$). The Am80-encapsulating micelles were prepared in the presence of DMDA
 447 at various molar ratios to Am80 (circle = 1, diamond = 5.4, and triangle = 10.7). The result
 448 at the ratio of 5.4 represented in Fig. 3 was shown again for the comparison with the
 449 results at the other ratios. The amounts of drug encapsulated in polymeric micelles were
 450 normalized to 100%.

445 DMDA/Am80 ratio of 1. This deficient retardation was probably due to
 446 the presence of the carboxyl group of polymer 4. This carboxyl group
 447 would compete with the carboxyl group of Am80 for interaction with
 448 DMDA. Therefore the excess amount of DMDA going to Am80 was
 449 necessary for the obvious retardation. In fact, the molar amount of
 450 DMDA at a DMDA/Am80 molar ratio of 5.4 in which the substantial
 451 retardation effect was demonstrated was equal to the molar amount of
 452 all the carboxyl groups of Am80 and polymer 4. Two mechanisms serve
 453 to explain the observed retardation, as shown in Fig. 5. The first is an
 454 increase in the hydrophobicity of Am80 caused by the ion-pairing with
 455 DMDA as described above. The second is a change of characteristics of
 456 the micelle inner core accompanying the pairing of the carboxyl group
 457 of polymer 4 and DMDA. It is difficult to indicate which mechanism
 458 dominantly contributed to the retardation, since the current study did
 459 not separate the effect on Am80 from that on the polymer.

460 Zeta potential of empty polymeric micelles except for the micelles
 461 of polymer 5 was -5.6 ± 0.2 to -12.6 ± 1.3 mV; see Supplementary
 462 Table S1. These values were slightly decreased with the Am80
 463 encapsulation (-9.9 ± 0.0 to -22.1 ± 0.7 mV). Although the DMDA
 464 addition raised the zeta potential, the micelles kept negative surface
 465 charges under the conditions for the retardation experiments of the
 466 Am80 release.

467 As described above, the addition of DMDA successfully triggered
 468 the retardation of the Am80 release. The presumption is that the
 469 triggering mechanism involved the hydrophobic complex formation
 470 between Am80 and DMDA, and the encapsulation of this complex in
 471 the polymeric micelle. Therefore, we investigated not only Am80 but
 472 also the co-encapsulation of DMDA into the polymeric micelle.

473 The polymeric micelle solutions prepared in the presence of Am80
 474 and DMDA were ultrafiltered with a Microcon YM-100 (100-kDa cut-
 475 off). This process separated the polymeric micelles in the retentate
 476 from low-molecular compositions in the filtrate. A retentate is a
 477 residual solution on an ultrafilter membrane after the ultrafiltration,
 478 and a filtrate is a solution that has passed through the ultrafilter. The
 479 amounts of Am80 and DMDA both in the retentate and the filtrate
 480 were measured by means of an HPLC. Six samples were applied to this
 481 separation experiment, as summarized in Table 4. The sample
 482 solutions included DMDA, polymer 1, and Am80 (Entry 1), DMDA
 483 alone (Entries 2 and 3), DMDA and polymer 1 (Entry 4), and DMDA
 484 and Am80 (Entries 5 and 6). We prepared the solutions by using the
 485 evaporation-sonication process.

486 Approximately 76% of the feed DMDA was recovered in the sample
 487 solutions prepared in the presence of polymer 1 and Am80 (Table 4; 487